

Co-evolution between the first supermassive black holes and their host galaxies

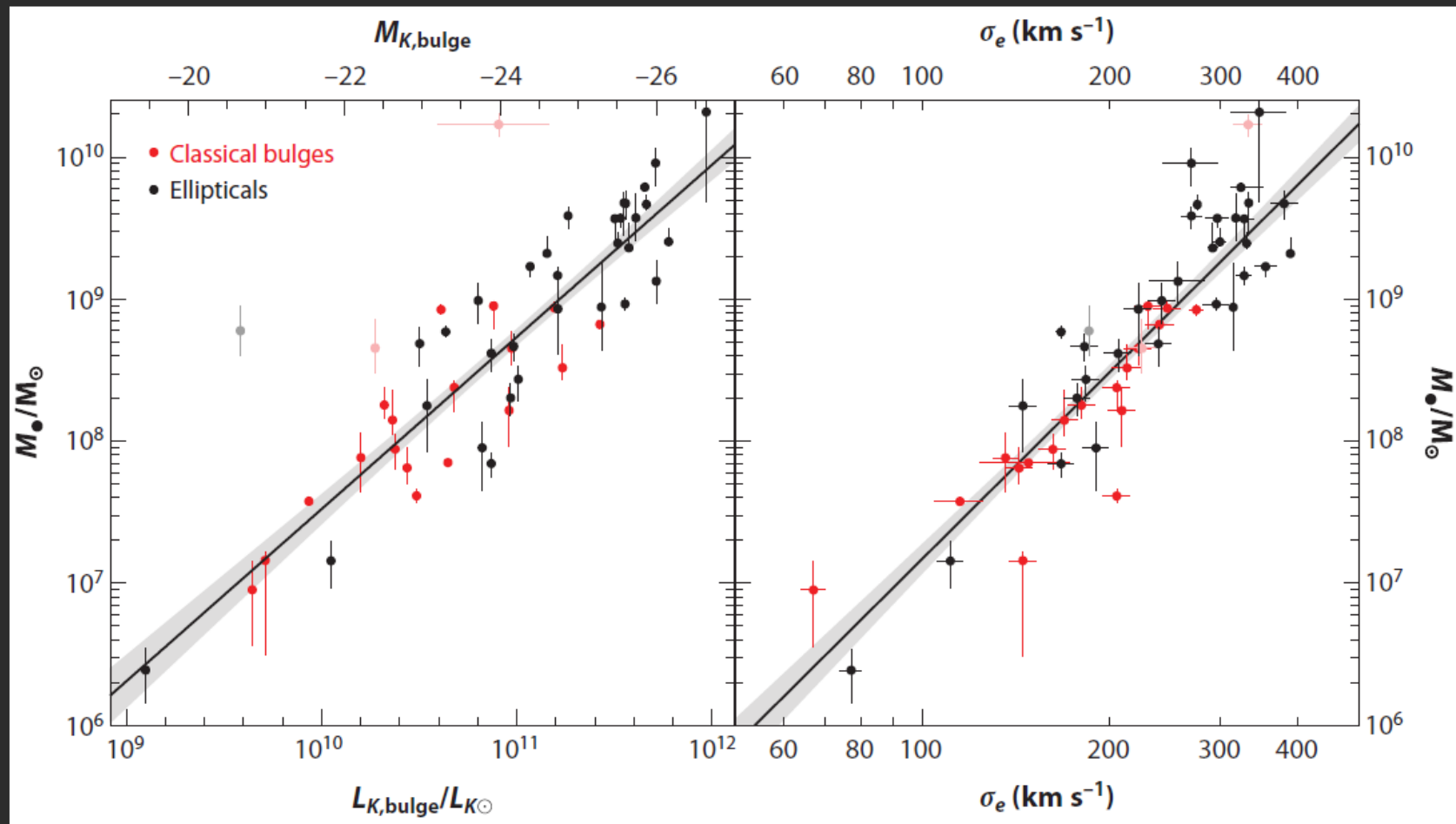
Ran Wang

KIAA–Peking University

2019. 11. 28

- **Collaborators:** Carilli, C. (NRAO); Walter, F. (MPIfA); Fan, X. (Steward); Wagg, J. (NRAO); Neri, R. (IRAM); Bertoldi, F. (University of Bonn); Riechers, D. (Caltech); Decarli, R. (INAF); Willott, C. (Herzberg Institute of Astrophysics); Omont, A. (IAP); Strauss, M. (Princeton); Cox, P. (IRAM); Menten, K. (MPIfR); Wu, X. (KIAA-PKU); Jiang, L. (KIAA-PKU); Yali Shao ; Qiong Li(PhD, PKU)

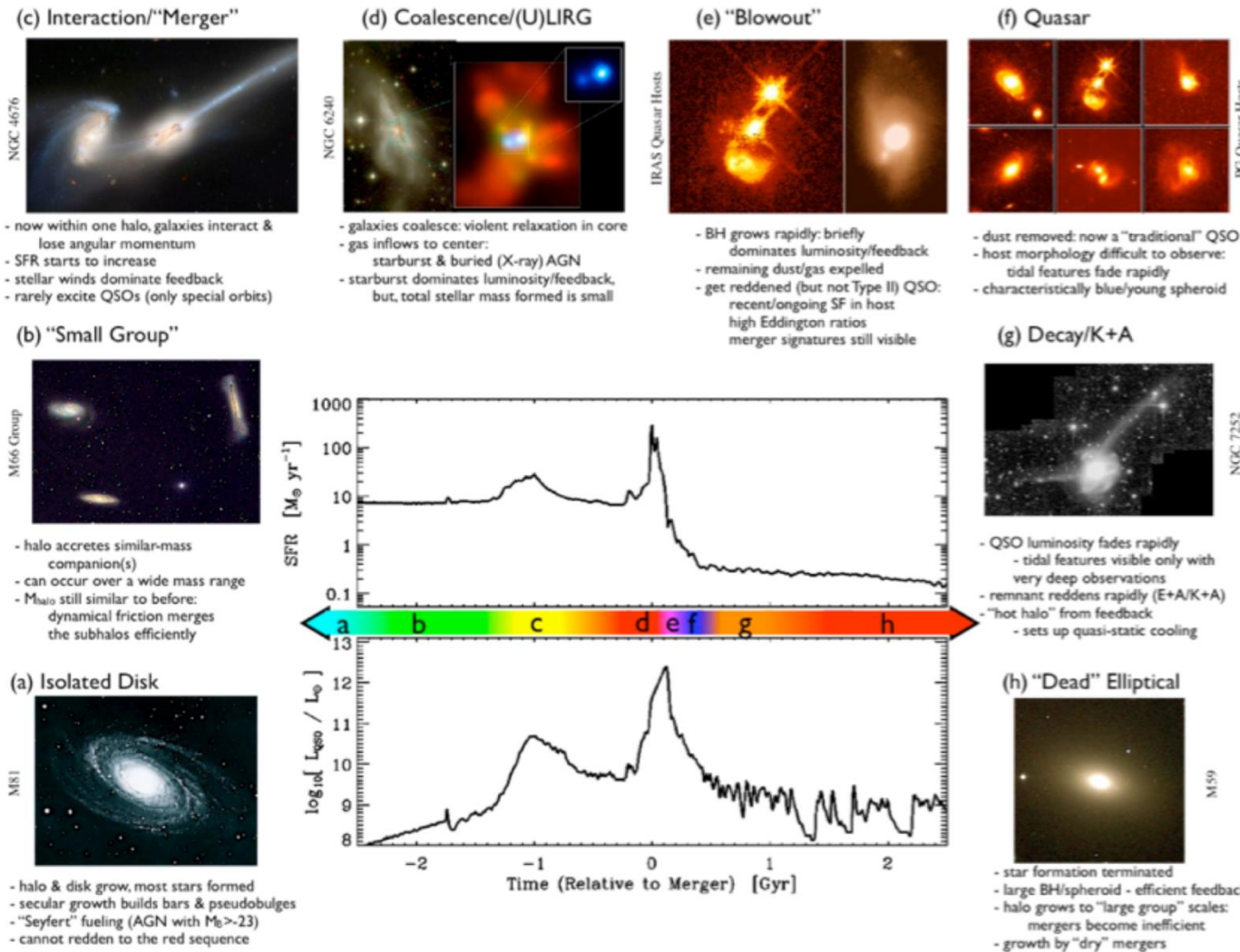
SMBH-galaxy co-evolution



Kormendy & Ho 2013

$$\frac{M_\bullet}{10^9 M_\odot} = (0.49_{-0.05}^{+0.06}) \left(\frac{M_{\text{bulge}}}{10^{11} M_\odot} \right)^{1.17 \pm 0.08} ; \quad \text{intrinsic scatter} = 0.28 \text{ dex.}$$

SMBH-galaxy co-evolution

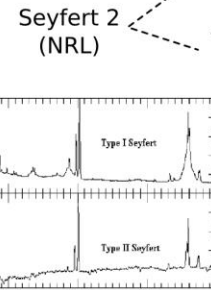


Credit: Hopkins et al. NSF

Blazar

FR-I

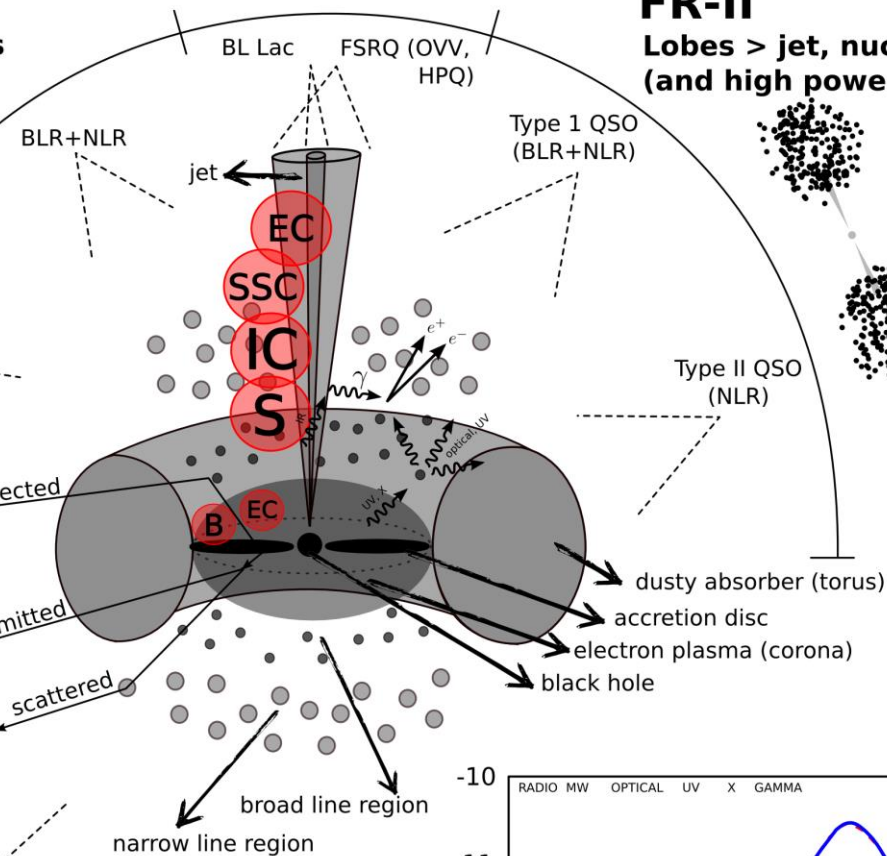
Lobes < jet, nucleus
(and low power)



from Ghisellini, 2012

FR-II

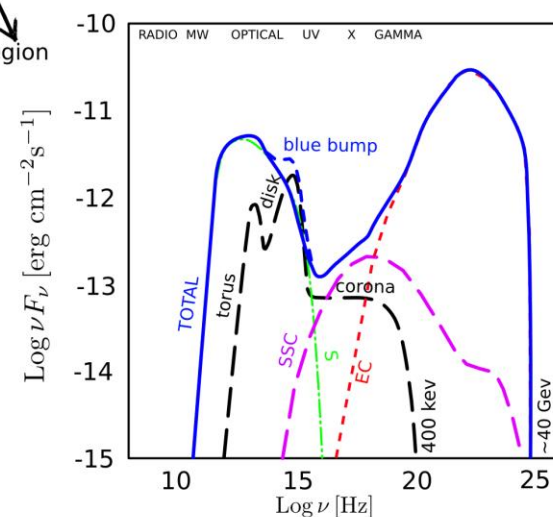
Lobes > jet, nucleus
(and high power)



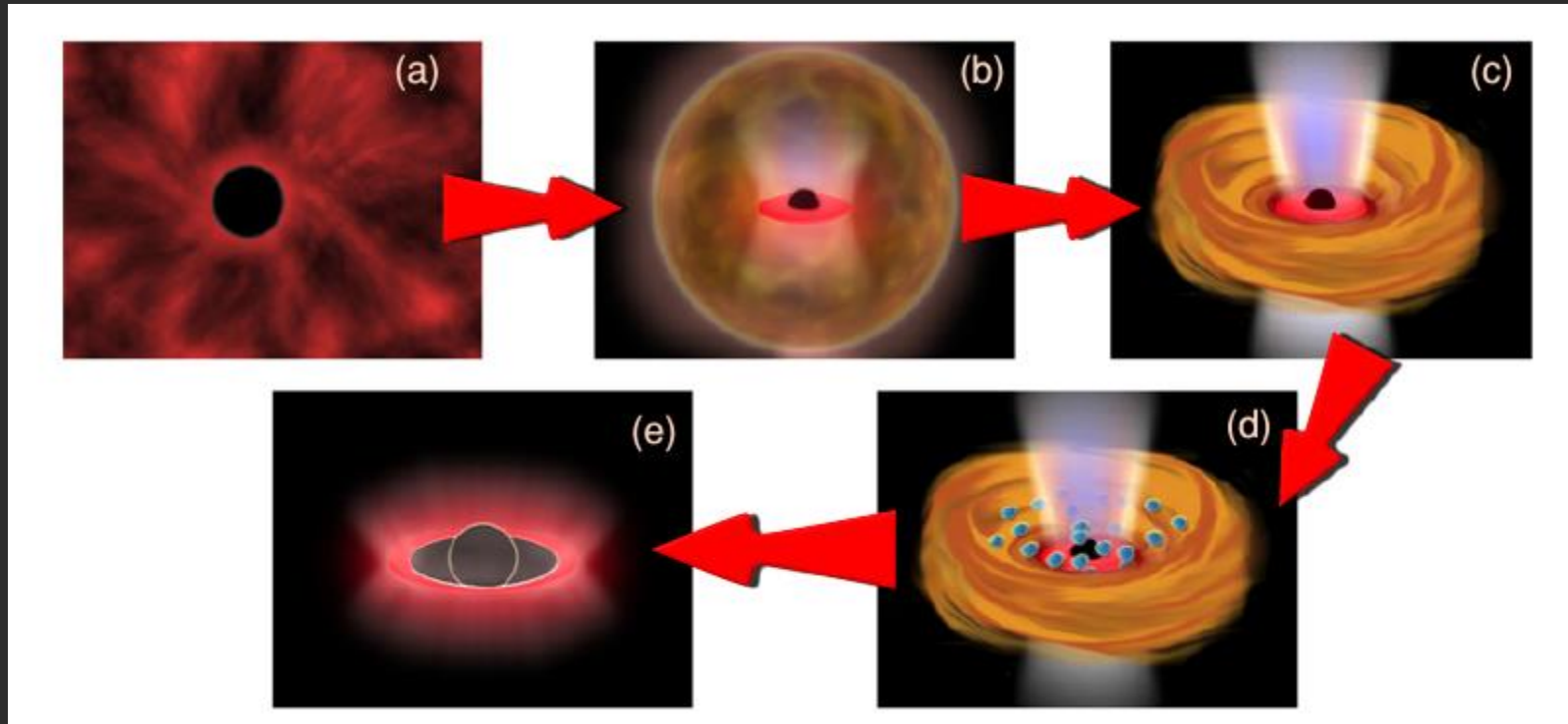
B = Bremsstrahlung
S = Synchrotron
C = Compton
IC = Inverse Compton
SSC = S self-Compton
EC = External Compton

Adapted from
 "Active Galactic Nuclei,
 Beckmann&Shrader"

AGN
 for
 Dummies



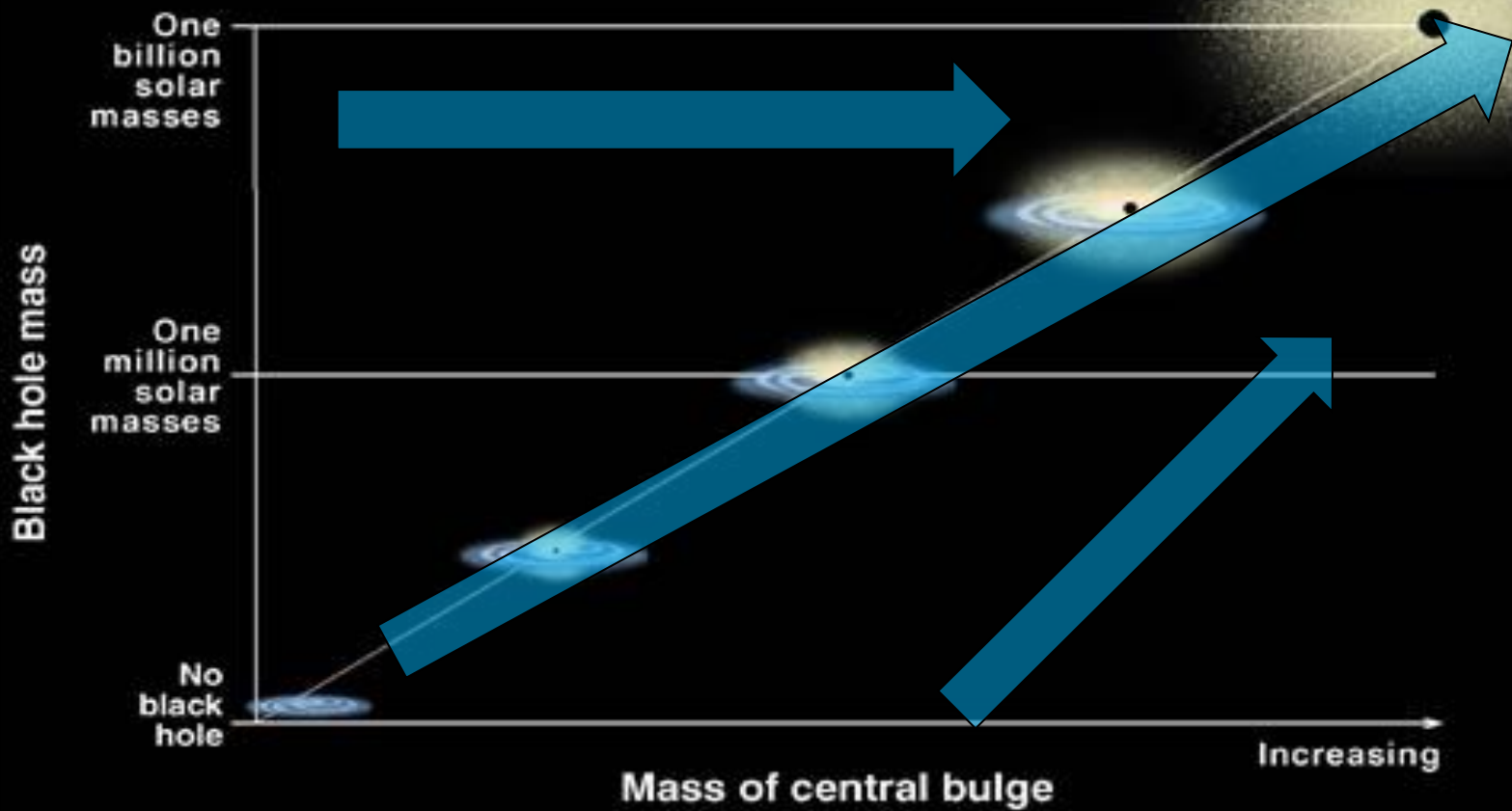
adapted from Ghisellini, 2012



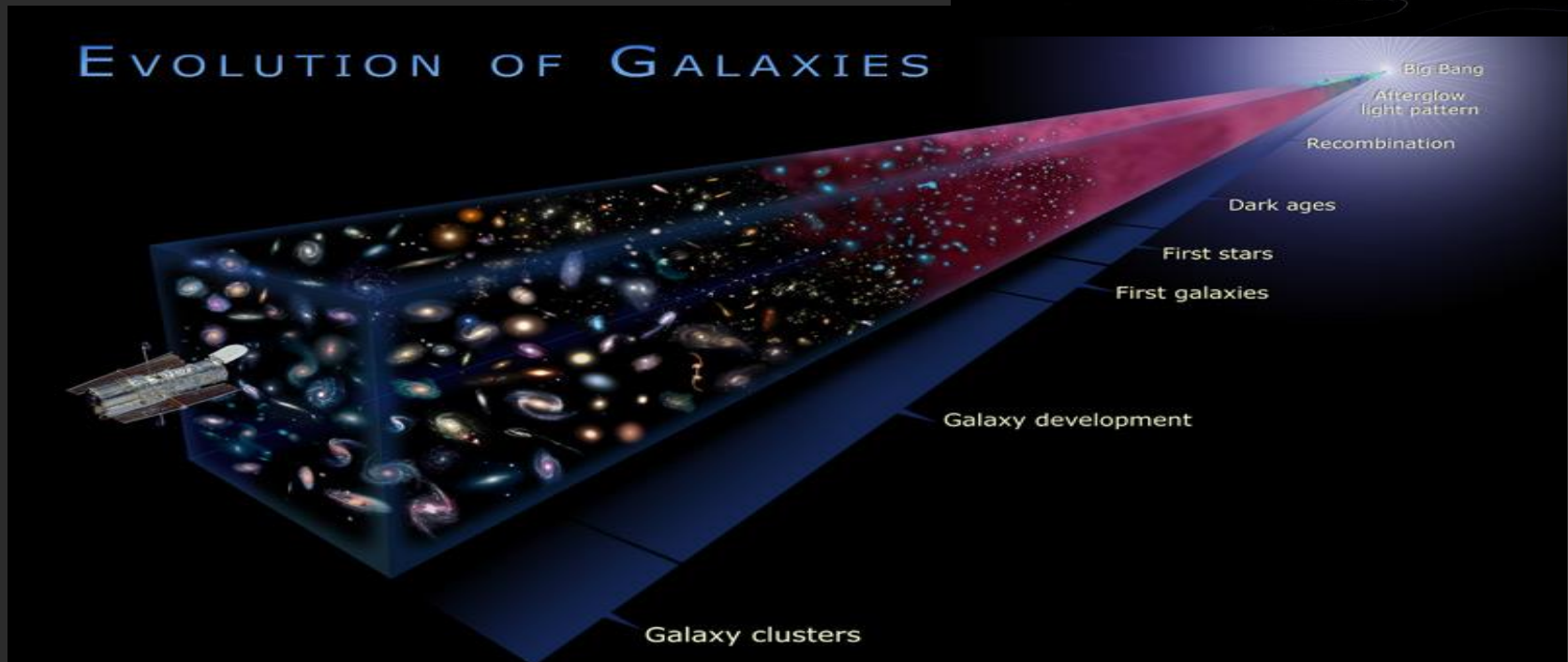
Liu & Zhang 2011

SMBH-galaxy co-evolution

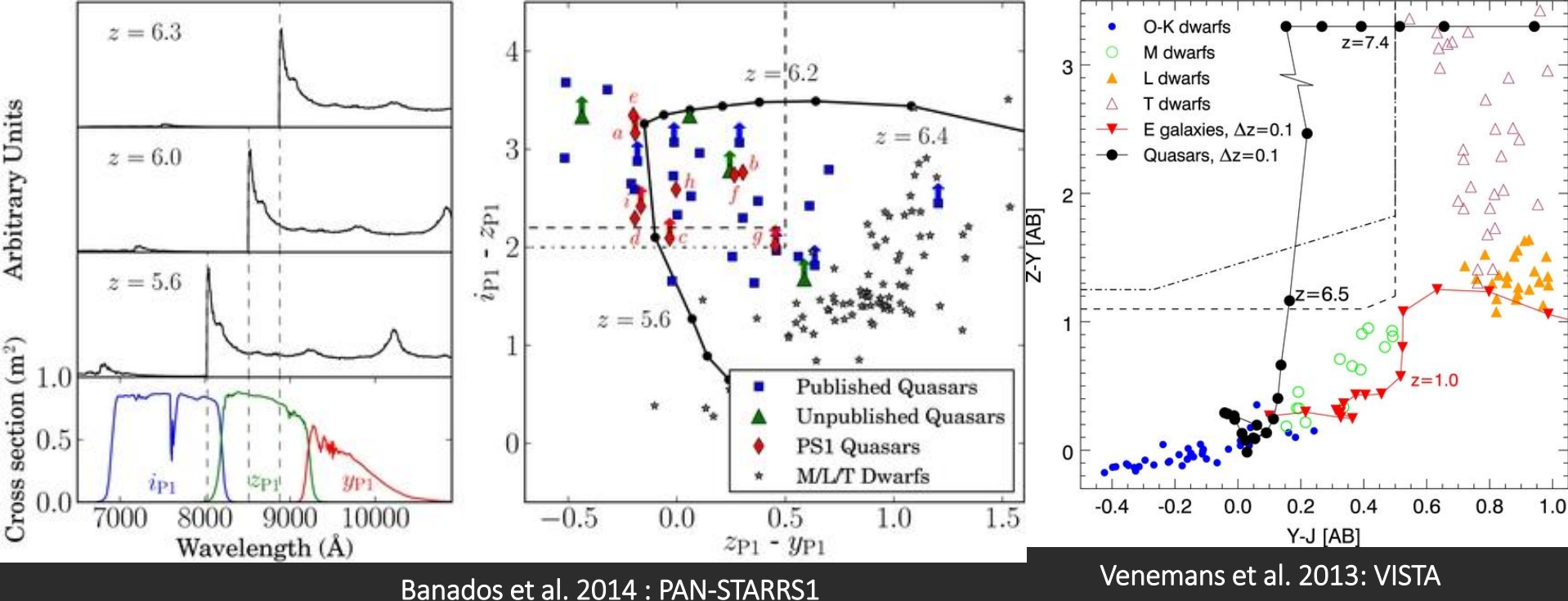
Correlation Between Black Hole Mass and Bulge Mass



Quasars discovered at the highest redshift



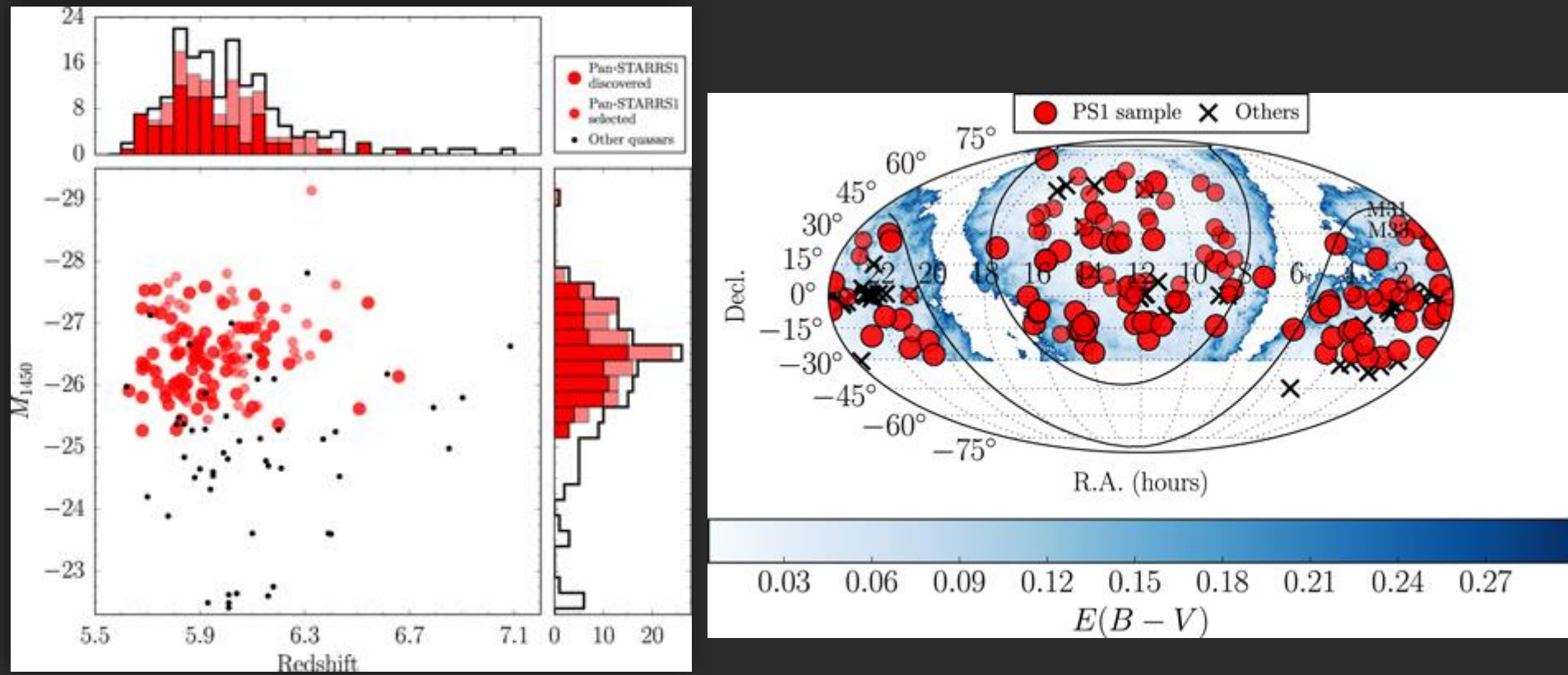
Quasars discovered at the highest redshift



- More than 180 quasars at $z > 5.7$ discovered from the large optical/near-IR surveys:
- SDSS main survey, $\text{mag_z} < 20.2$, Fan et al. 2000~2006
- SDSS stripe 82, Jiang et al. 2008, 2009; CFHQS, Willott et al. 2007-2010; UKIDSS, Mortlock et al. 2011; VISTA, Venemans et al. 2013; PAN-STARRS1, Banados et al. 2014; Venemans et al. 2013, 2015, Banados et al. 2016; Subaru: Matsuoka et al. 2017

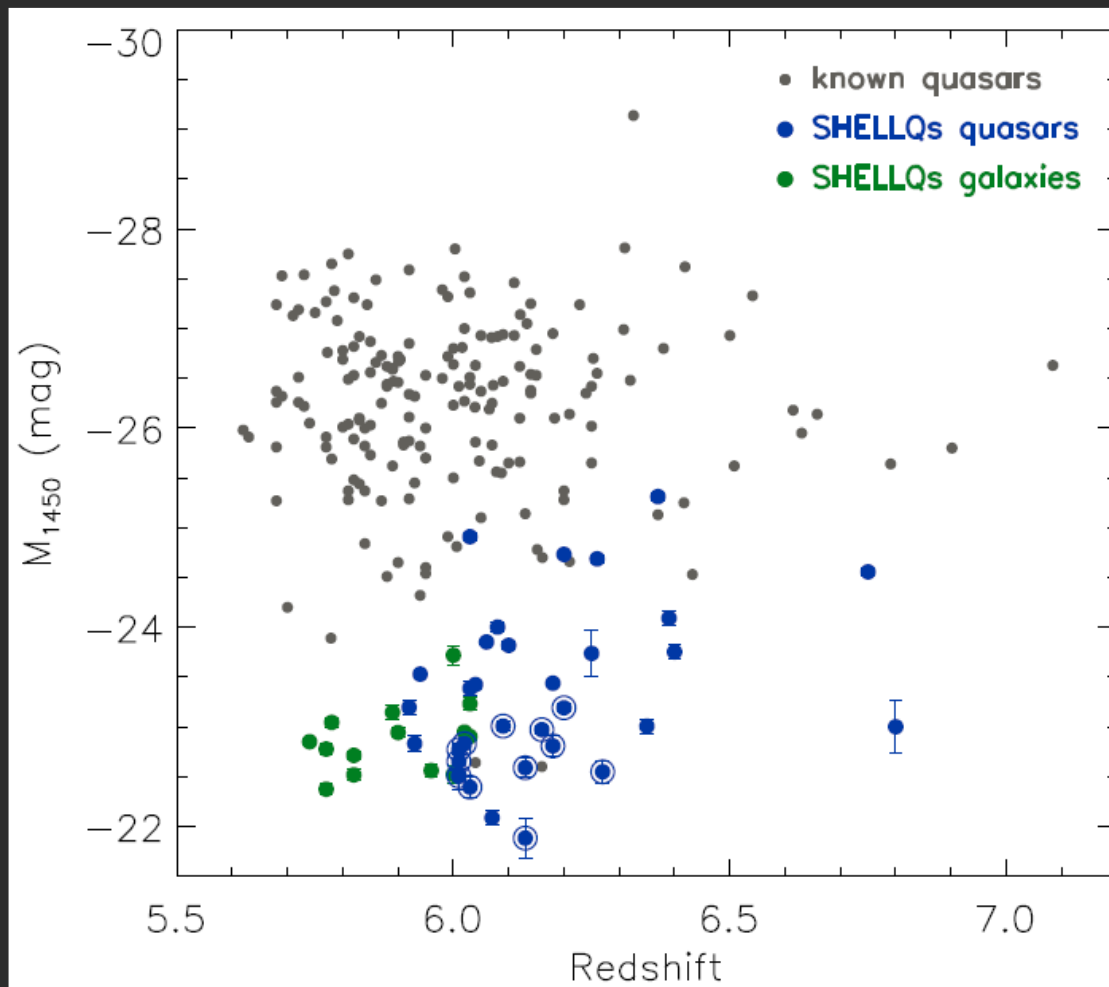
Introduction: Discovery of highest- z quasars

- More than 180 quasars at $z > 5.6$ discovered from the large optical/near-IR surveys: SDSS, Pan-STARRS1, CFHQS, etc.
recent summary from Banados et al. 2016, ApJS, 227, 11



Introduction: Discovery of highest-z quasars

- Fainter objects, less luminous and more common population at the highest redshift : Subaru SHELLQs, etc. (Matsuoka et al. 2017, PASJ)

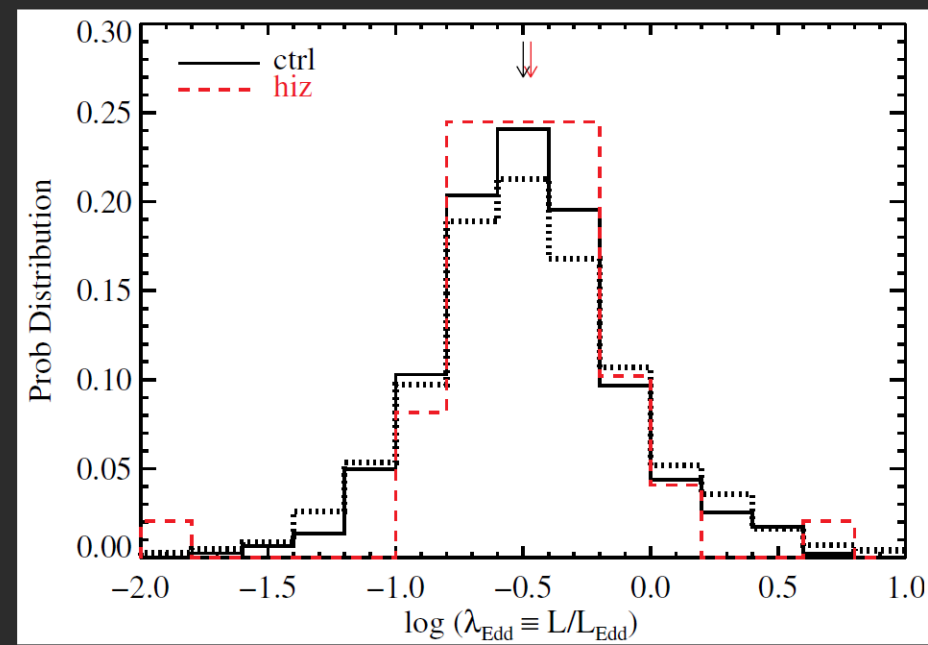
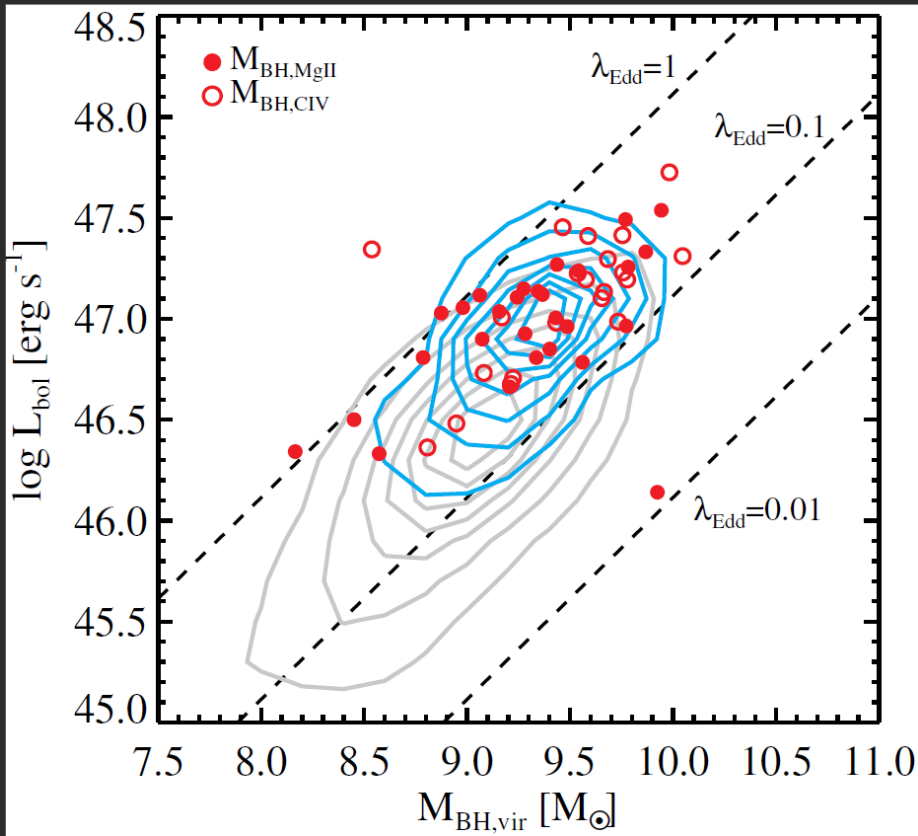


Quasars discovered at the highest redshift

- More than 200 quasars at $z > 5.7$ discovered from the large optical/near-IR surveys:
- SDSS main survey, $\text{mag_z} < 20.2$, Fan et al. 2000~2006
- SDSS stripe 82, Jiang et al. 2008, 2009; CFHQS, Willott et al. 2007-2010; UKIDSS, Mortlock et al. 2011; VISTA, Venemans et al. 2013; PAN-STARRS1, Banados et al. 2014; Venemans et al. 2013, 2015, Banados et al. 2016; Subaru: Matsuoka et al. 2017, 2019;
- Fainter objects, less luminous and more common population at the highest redshift : Subaru SHELLQs, etc. (Matsuoka et al. 2017, 2019, PASJ)

Quasars discovered at the highest redshift

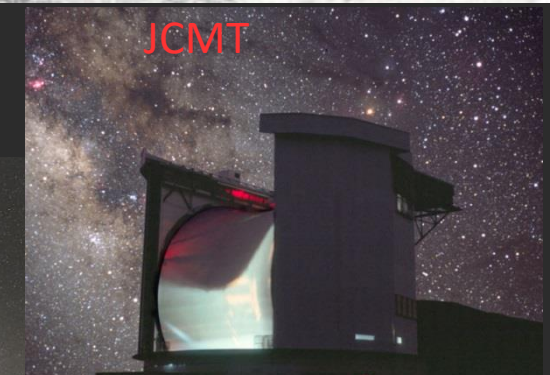
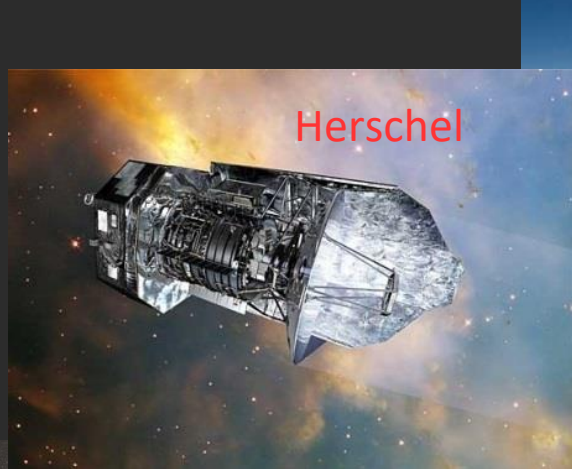
- Quasar activities : similar to the low-z quasars in similar luminosity range (Shen et al. 2019).



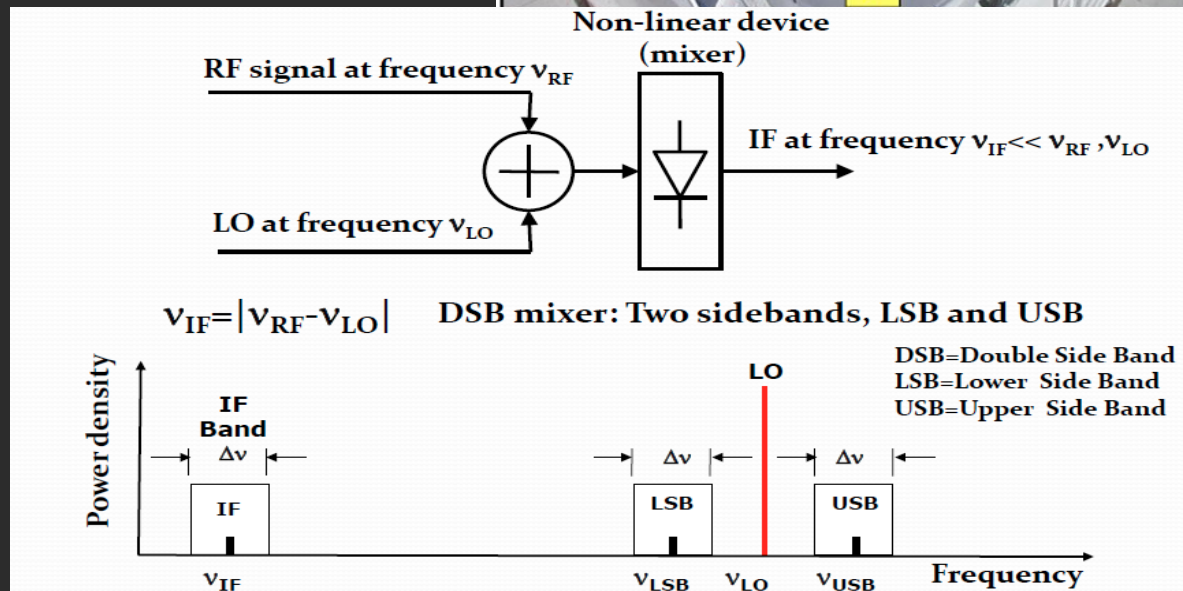
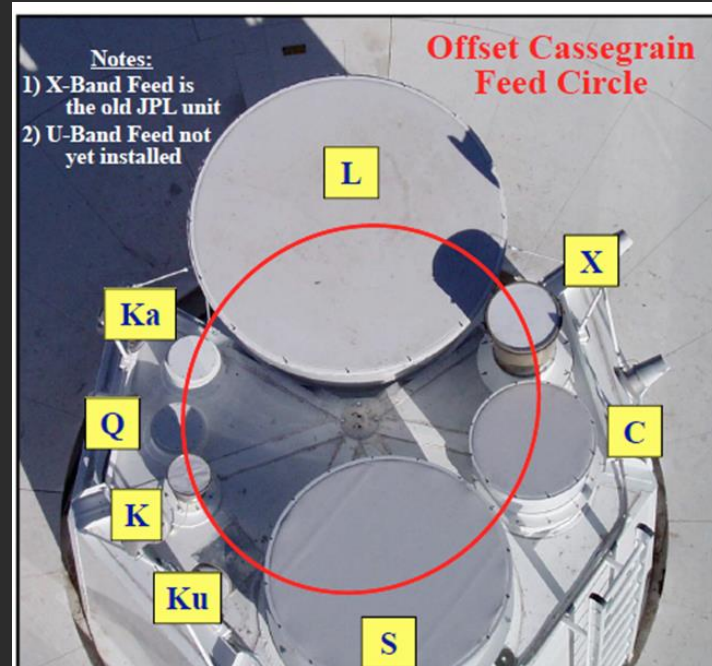
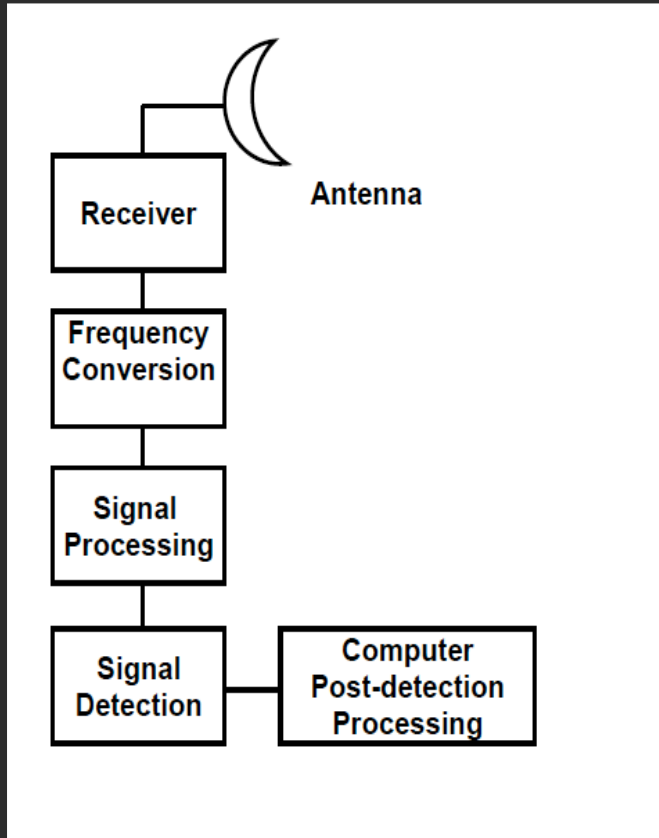
The millimeter and radio telescopes



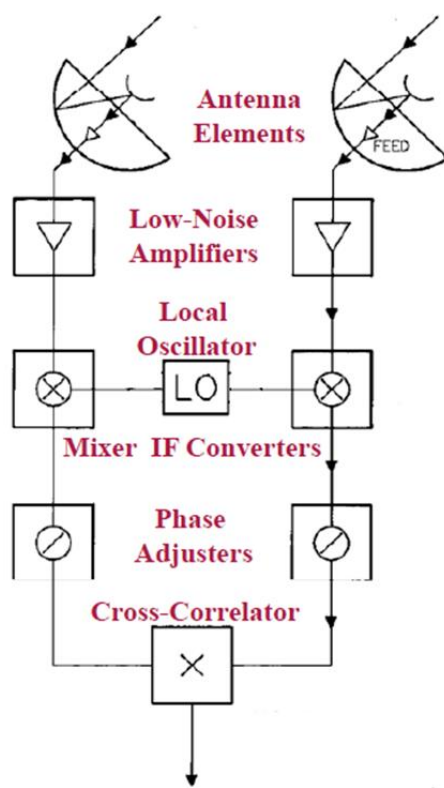
NOEMA



Heterodyne receivers



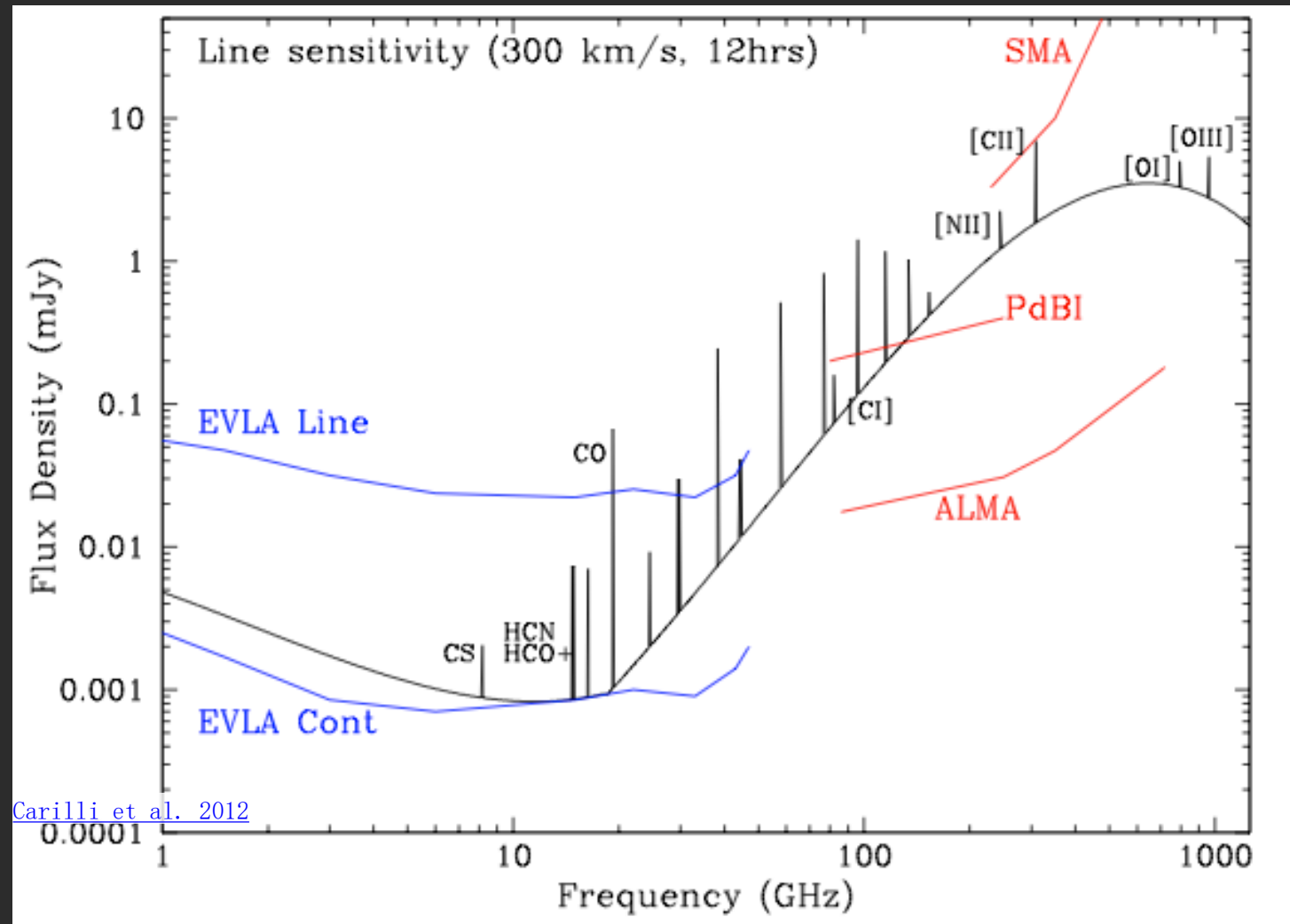
ALMA: Best sensitivity: Spatial resolution.



Specification	
<i>Number of Antennas</i>	<i>At least 50×12-m (12-m Array), plus 12×7-m & 4×12-m (ACA)</i>
<i>Maximum Baseline Lengths</i>	<i>0.15 - 16 km</i>
<i>Angular Resolution (")</i>	<i>~0.2" × (300/ν GHz) × (1 km / max. baseline)</i>
<i>12-m Primary beam (")</i>	<i>~20.6" × (300/ν GHz)</i>
<i>7-m Primary beam (")</i>	<i>~35" × (300/ν GHz)</i>
<i>Number of Baselines</i>	<i>Up to 1225 (ALMA correlator can handle up to 64 antennas)</i>
<i>Total Bandwidth</i>	<i>16 GHz (2 polarizations × 4 basebands × 2 GHz/baseband)</i>
<i>Velocity Resolution</i>	<i>As narrow as $0.008 \times (\nu/300 \text{ GHz}) \text{ km/s}$</i>
<i>Polarimetry</i>	<i>Full Stokes parameters</i>

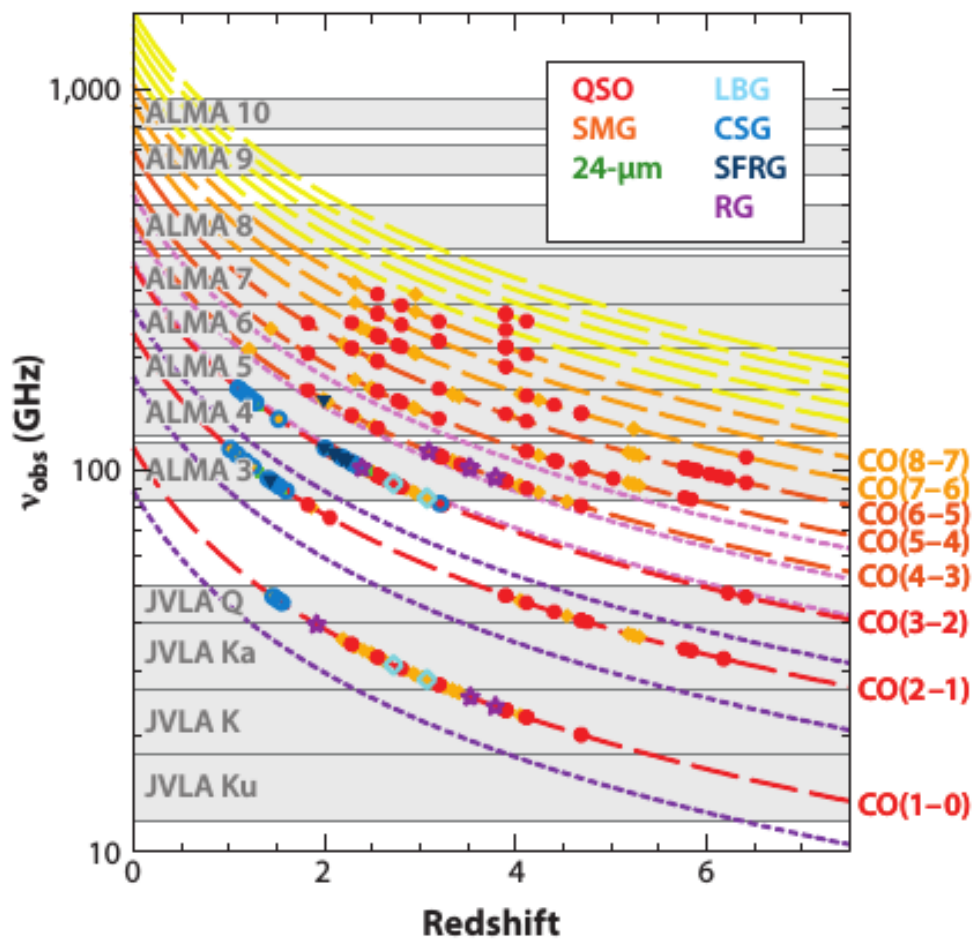
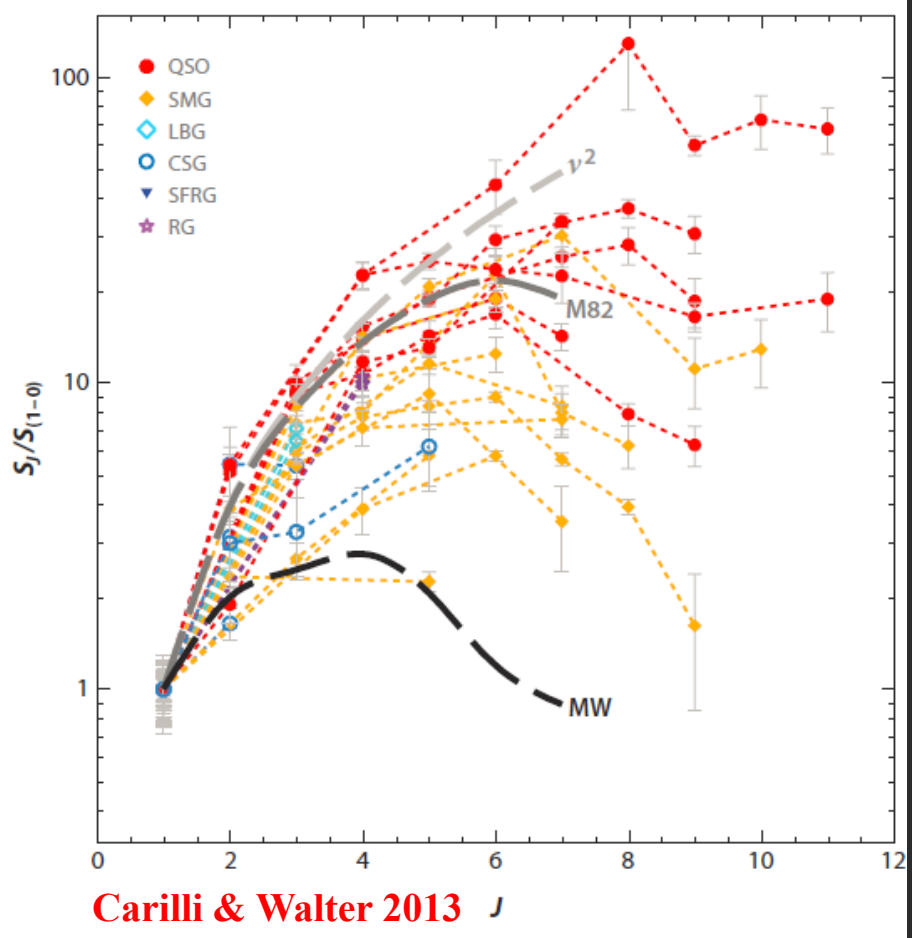
Full Science Capabilities						Most Compact		Most Extended	
Band	Frequency (GHz)	Wavelength (mm)	Primary Beam (FOV; ")	Approx. Max. Scale (")	Continuum Sensitivity (mJy/beam)	Angular Resolution (")	ΔT _{line} (K)	Angular Resolution (")	ΔT _{line} (K)
1*	31.3-45	6.7-9.5	145-135	93	‡	13-9	‡	0.14-0.1	‡
2*	67-90	3.3-4.5	91-68	53	‡	6-4.5	‡	0.07-0.05	‡
3	84-116	2.6-3.6	72-52	37	0.07	4.9-3.6	0.04	0.05-0.038	430
4	125-163	1.8-2.4	49-37	32	0.06	3.3-2.5	0.048	0.035-0.027	330
5	163-211	1.4-1.8	37-29	23	*	*	*	*	*
6	211-275	1.1-1.4	29-22	18	0.09	2.0-1.5	0.05	0.021-0.016	490
7	275-373	0.8-1.1	22-16	12	0.15	1.5-1.1	0.08	0.016-0.012	814
8	385-500	0.6-0.8	16-12	9	0.40	1.07-0.82	0.28	0.011-0.009	1900
9	602-720	0.4-0.5	10-8.5	6	1.4	0.68-0.57	0.9	0.007-0.006	8900
10	787-950	0.3-0.4	7.7-6.4	5	1.2	0.52-0.43	1.6	0.006-0.005	—

Star forming galaxies at high redshift



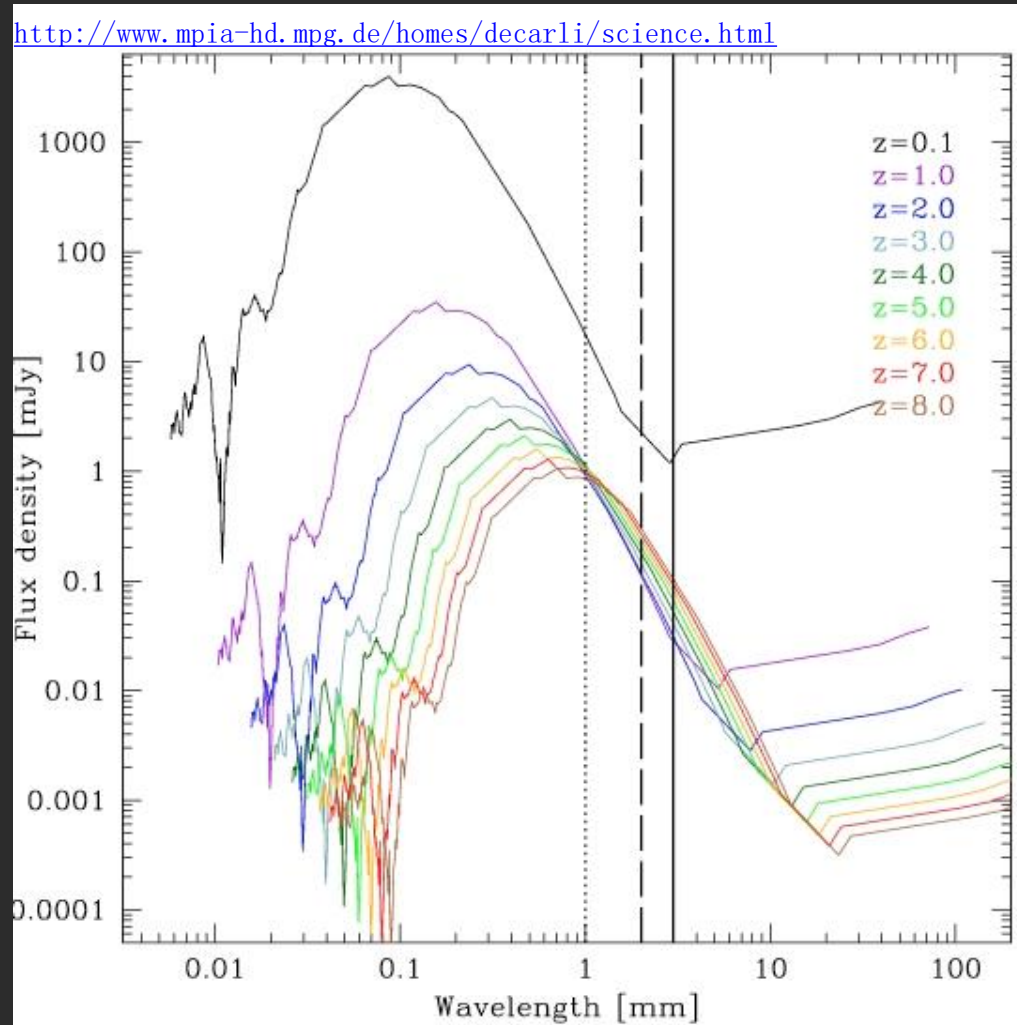


- Quasar host galaxies at the very high redshift, Molecular CO lines :



The negative K-correction and dust emission at high-z

- $L_{\text{fir}} \sim 4.7 \times 10^{12} (S_{250\text{GHz}} / \text{mJy}) L_{\text{sun}}$ at $z \sim 2$;
- $L_{\text{fir}} \sim 3.6 \times 10^{12} (S_{250\text{GHz}} / \text{mJy}) L_{\text{sun}}$ at $z \sim 4$;
- $L_{\text{fir}} \sim 2.34 \times 10^{12} (S_{250\text{GHz}} / \text{mJy}) L_{\text{sun}}$ at $z \sim 6$;



Millimeter and radio observations of the earliest quasar host galaxies

- Submm/mm continuum : redshifted FIR thermal dust continuum emission, 40~60 K, usually heated by nearby star formation;
- Molecular CO : direct tracer of the molecular gas;
- [C II] fine structure line : tracer of star formation, atomic and ionized gas;
- Interferometer observations :
 - Resolve the distributions of the dust, gas components and star formation activity;
 - Spectral lines : resolve the velocity field of the gas.

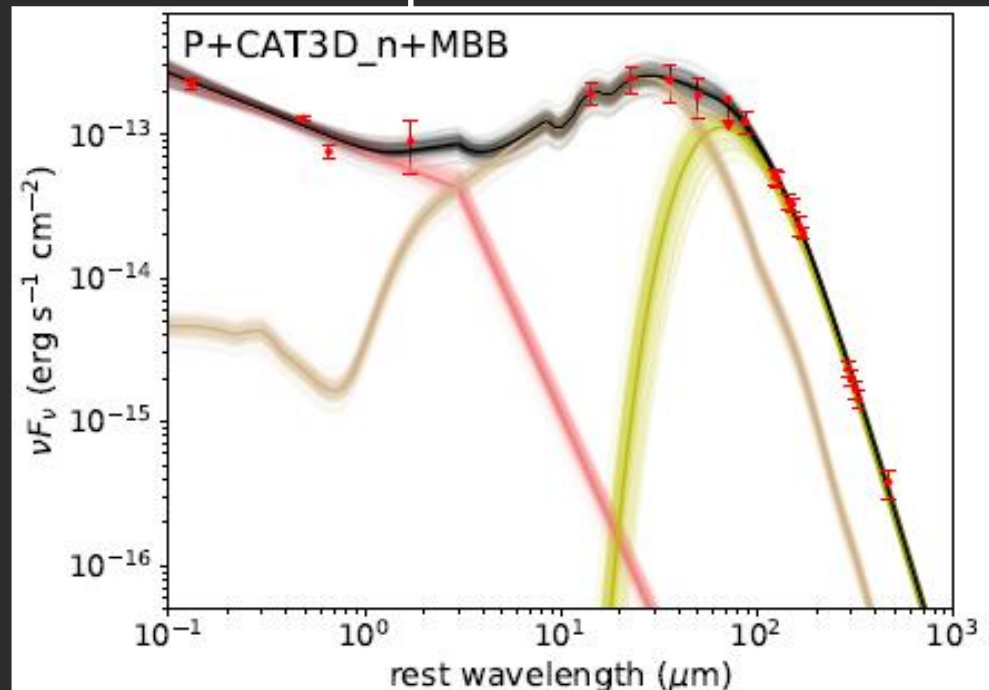
Questions on SMBH-galaxy formation

- Star formation co-eval with SMBH accretion ?
 - Searching for 40~60 K warm dust, [C II], molecular CO in the quasar host galaxies;
- Size, distribution of star formation ?
 - Mapping of the tracers of star formation, e.g., [C II];
 - Resolving the intense star formation in the nuclear region of a few kpc scale.
- Star formation rate ?
 - Questions of dust SED decomposition, IMF, etc.
- AGN feedback ?
 - Gas kinematics, outflows;
 - ISM excitation ;
- Masses of dust, gas, and stellar components, SMBH-host relations

Star formation: Dust and [C II] surveys

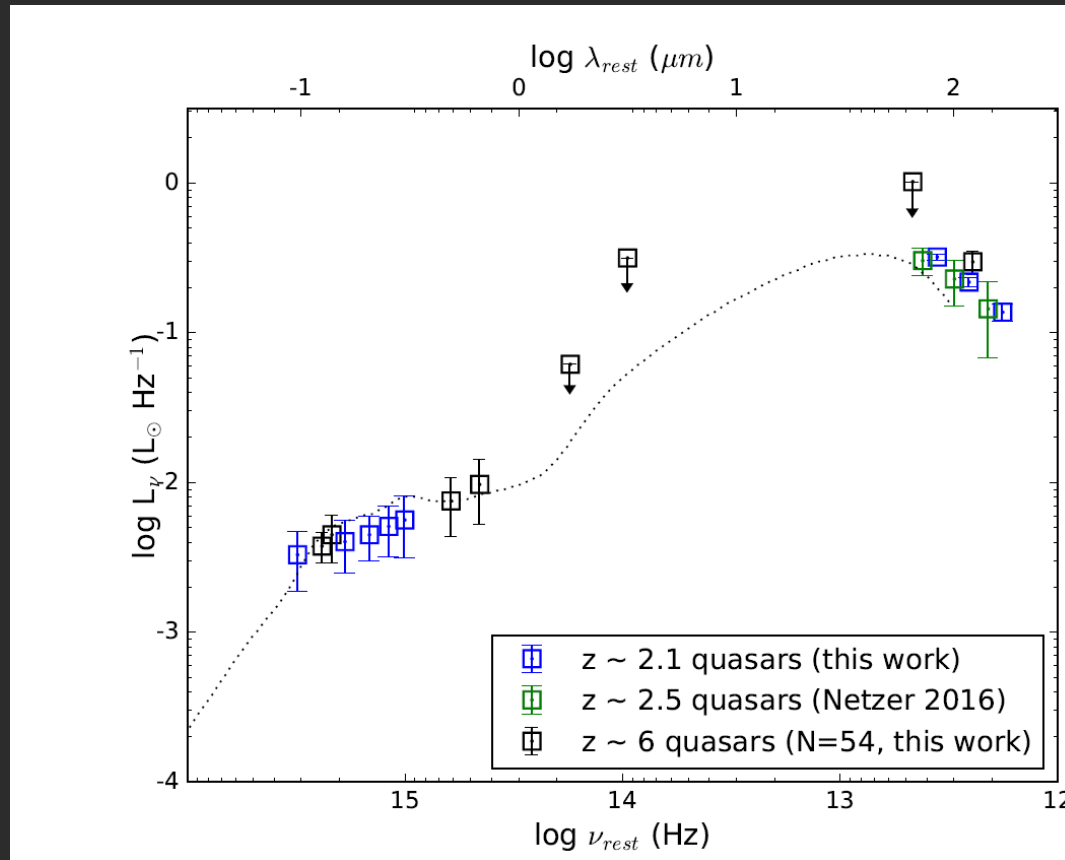
- Bright FIR dust continuum was first detected in $\sim 30\%$ of the optically luminous quasars at $z \sim 6$ using the JCMT, IRAM-30m;
- Combine of Herschel, IRAM, JCMT data: FIR emission powered by massive star formation in quasar hosts.
- FIR luminosities and Star formation rates comparable to ULIRGs or HLIRGs.

Right : the SED of a $z=6$ Quasar J2310 with $T_{\text{dust}} \sim 40 \text{ K}$



Star formation: Dust and [C II] surveys

- No clear evolution on the average optical to FIR SED of quasars from low- z to $z \sim 6$.
- JCMT SCUBA-2 survey of 54 $z \sim 6$ quasars by Qiong Li et al. 2019, in prep.



Recent ALMA programs of $z>6$ quasars by our and other groups

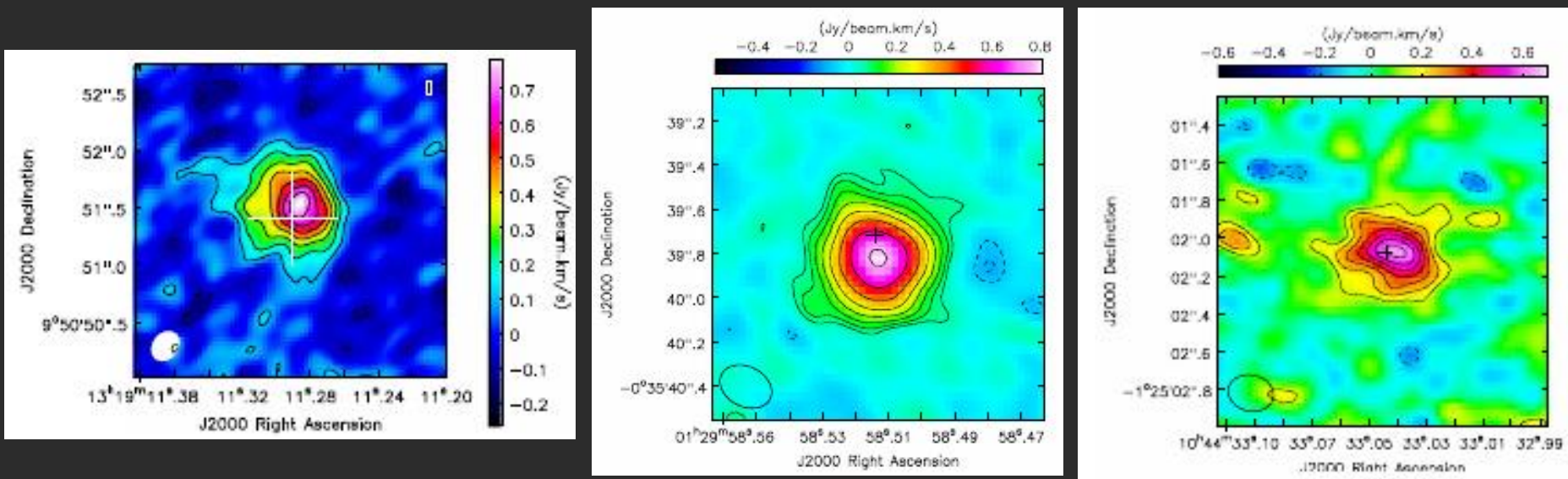
- The ALMA observations mainly focus on the [C II] 158 micron fine structure line and dust continuum:
 - Surveys of optically/mm-selected sample: sub-arcsec resolution, to constrain the source size and total fluxes;
 - [C II] emission from the sources that are bright in dust continuum from previous mm surveys, e.g., ALMA Cycle 0 Wang et al. (2013);
 - ALMA survey of optically selected $z>6$ quasars with $M_{1450} < -25.25$, Decarli et al. 2018: 27 objects at $z>6$, 100% detected in continuum and 85% in [C II];
 - ALMA observations of the optically fainter quasars discovered from HSC (Izumi et al. 2018, 2019)

Recent ALMA programs of $z>6$ quasars by our and other groups

- Continuum sensitivity 5~10 times deeper than previous single dish surveys;
- FIR luminosities $3 \times 10^{11} L_{\odot} \sim 10^{13} L_{\odot}$;
- Dust mass from $2 \times 10^7 \sim 10^9 M_{\odot}$.
- Detailed studies of the most [C II] luminous objects;
 - $0.1'' \sim 0.3''$ resolution imaging (e.g. Shao et al. 2017, Wang et al. 2019);
 - Observations of CO and other fine structure lines (e.g., Venemans et al. 2017; Carniani et al. 2019);

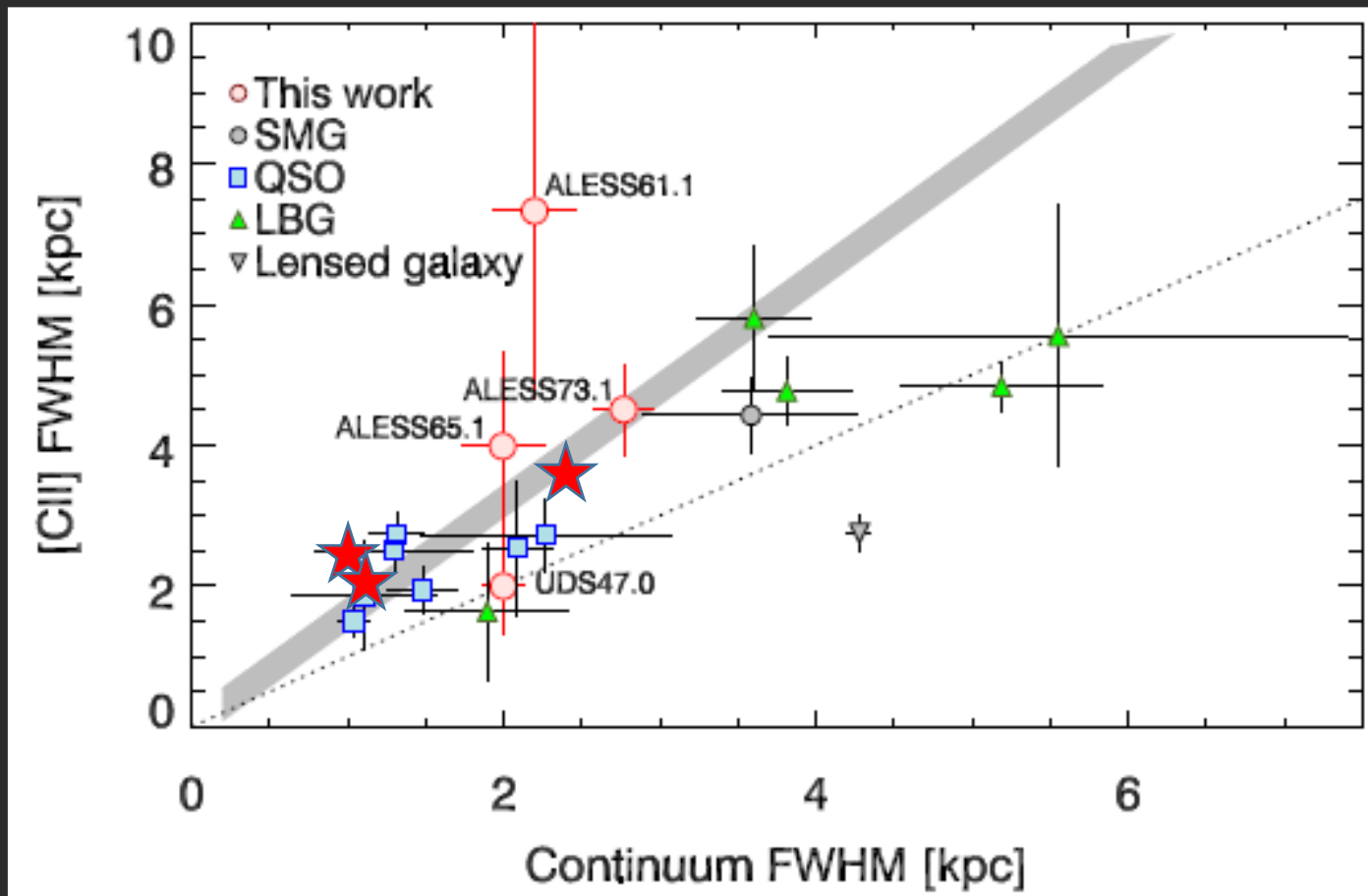
Dust and [C II] mapping on kpc scale

- ALMA observation of three $z \sim 6$ quasars at $0.2''$ resolution; Wang et al. 2019
- FWHM Source sizes : [C II] $0.3'' \sim 0.6''$ or 1.8 kpc ~ 3.6 kpc;
- The continuum emission is usually more compact;



Shao et al. 2017; Wang et al. 2019)

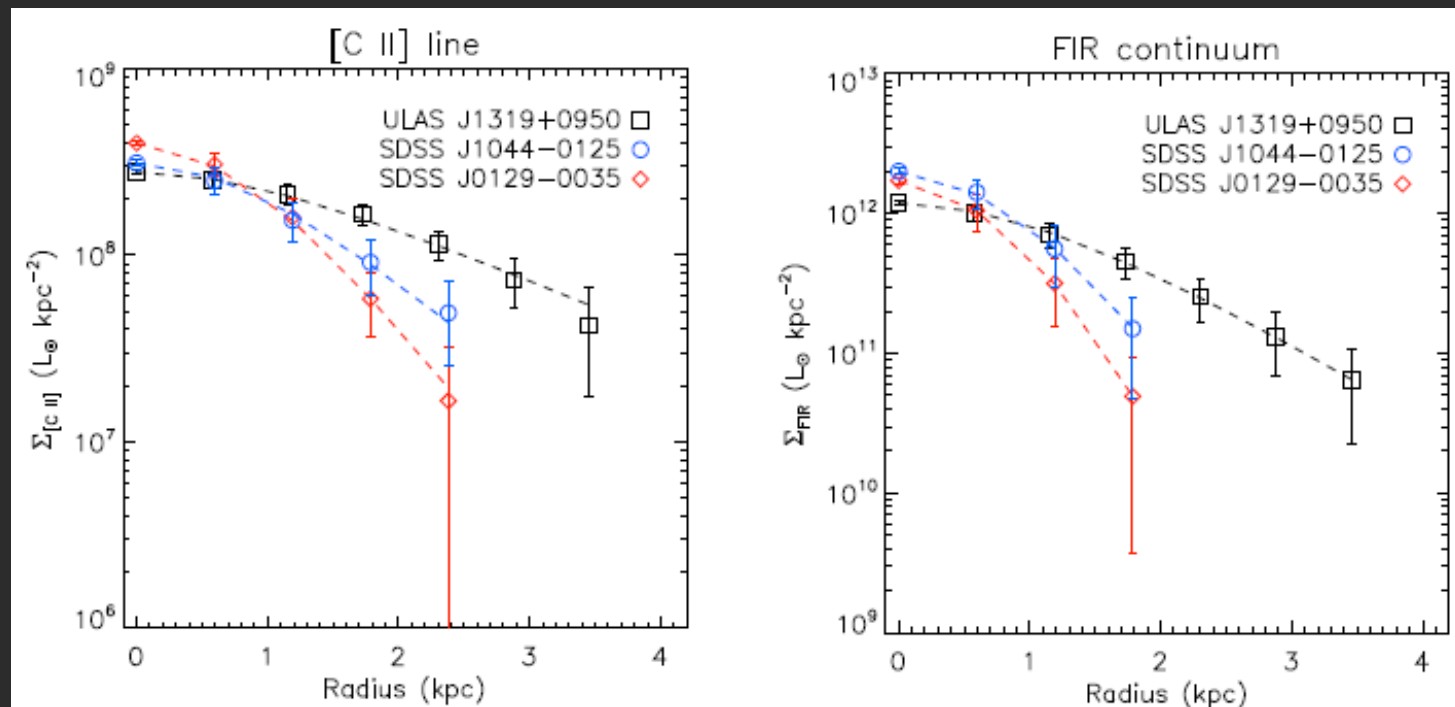
- Following the trend defined by other SMGs and quasars at lower redshift (Gullberg et al. 2018).



Adopted from Gullberg et al. 2018

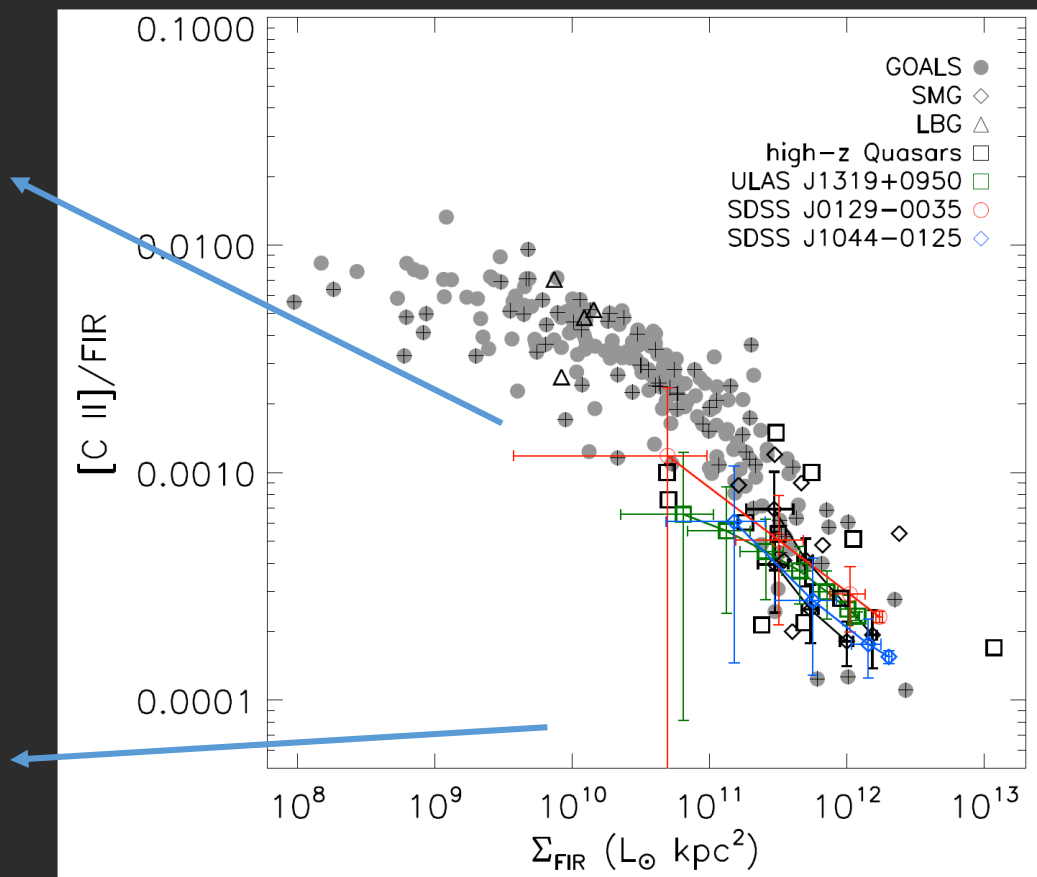
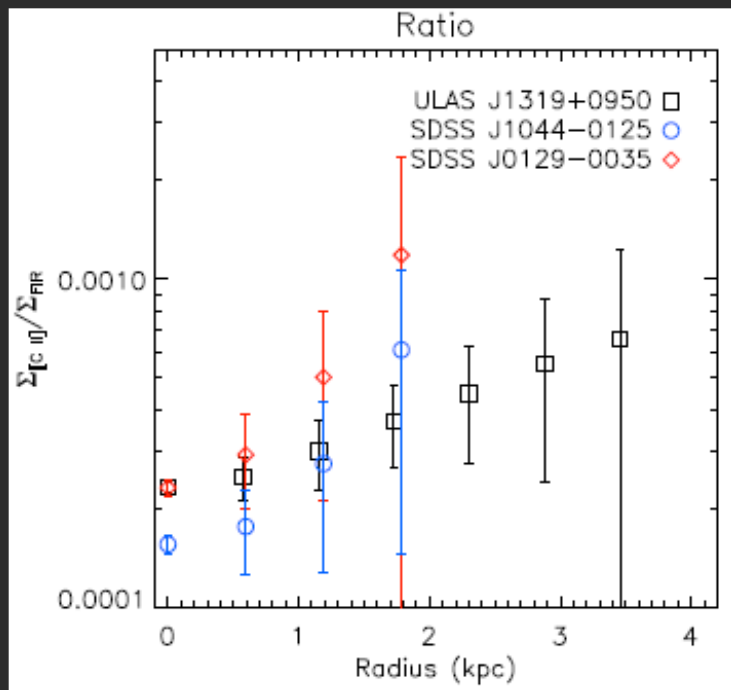
- Surface brightness vs. radius of [C II] and dust continuum: consistent with exponential light profiles;

Wang et al. 2019



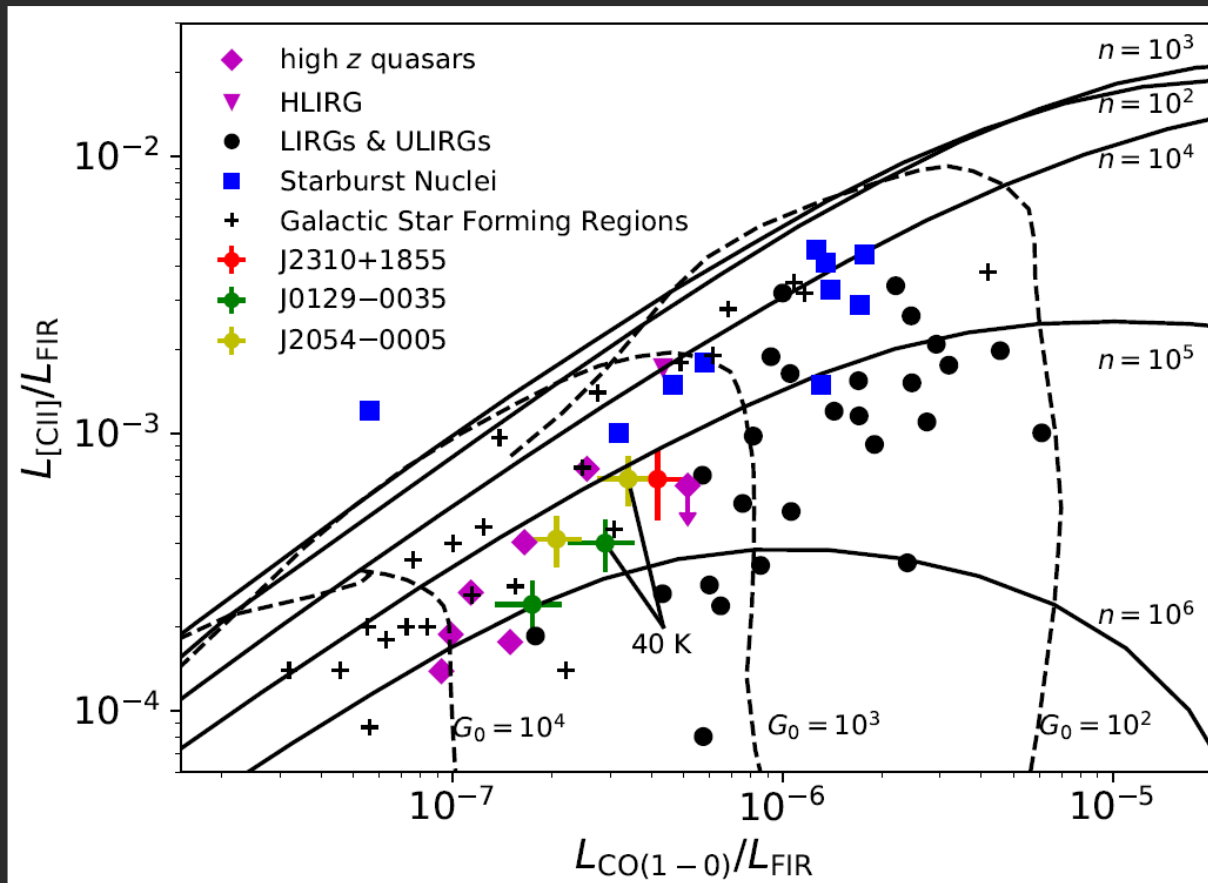
[CII] to FIR intensity ratio over the disk

- The FIR surface brightnesses in the nuclear region of all three objects are in the range between a few 10^{10} to 2×10^{12} $L_{\odot} \text{ kpc}^{-2}$, indicating a high density and dusty ISM with strong radiation field which could result in the low [C II]-to-FIR ratios



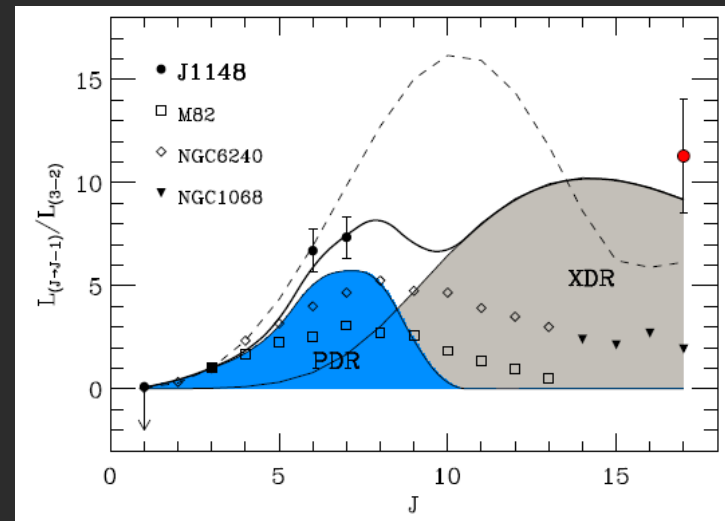
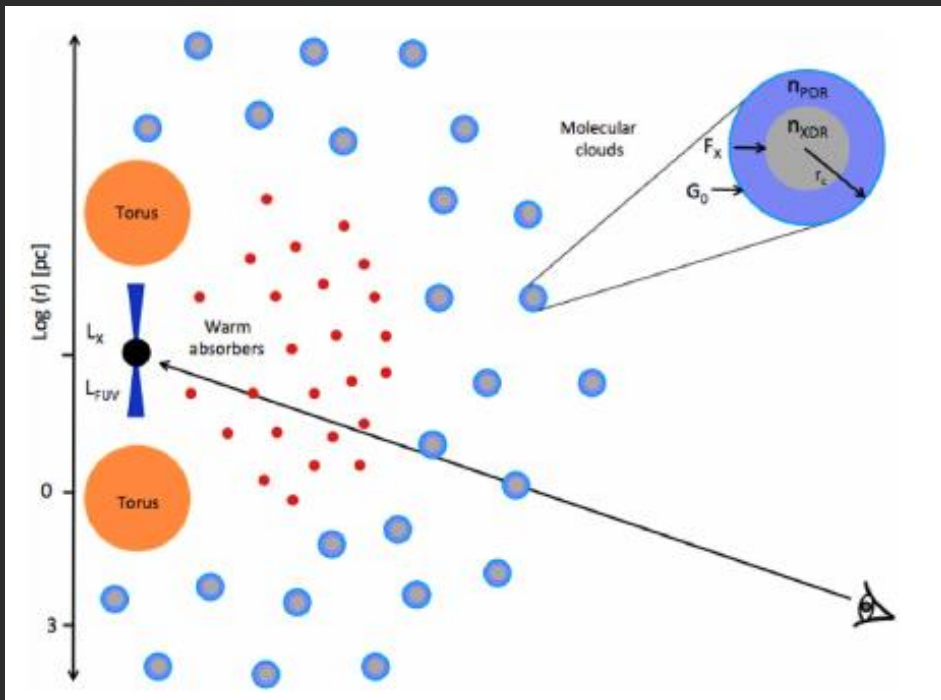
Physical condition and excitation of the ISM

- [C II] , low/mid-J CO suggest emission from PDR regions powered by star formation (Venemans et al. 2017; Shao et al. 2019)



Physical condition and excitation of the ISM

- Detections of very high- J CO suggest CO excitation by the central AGN

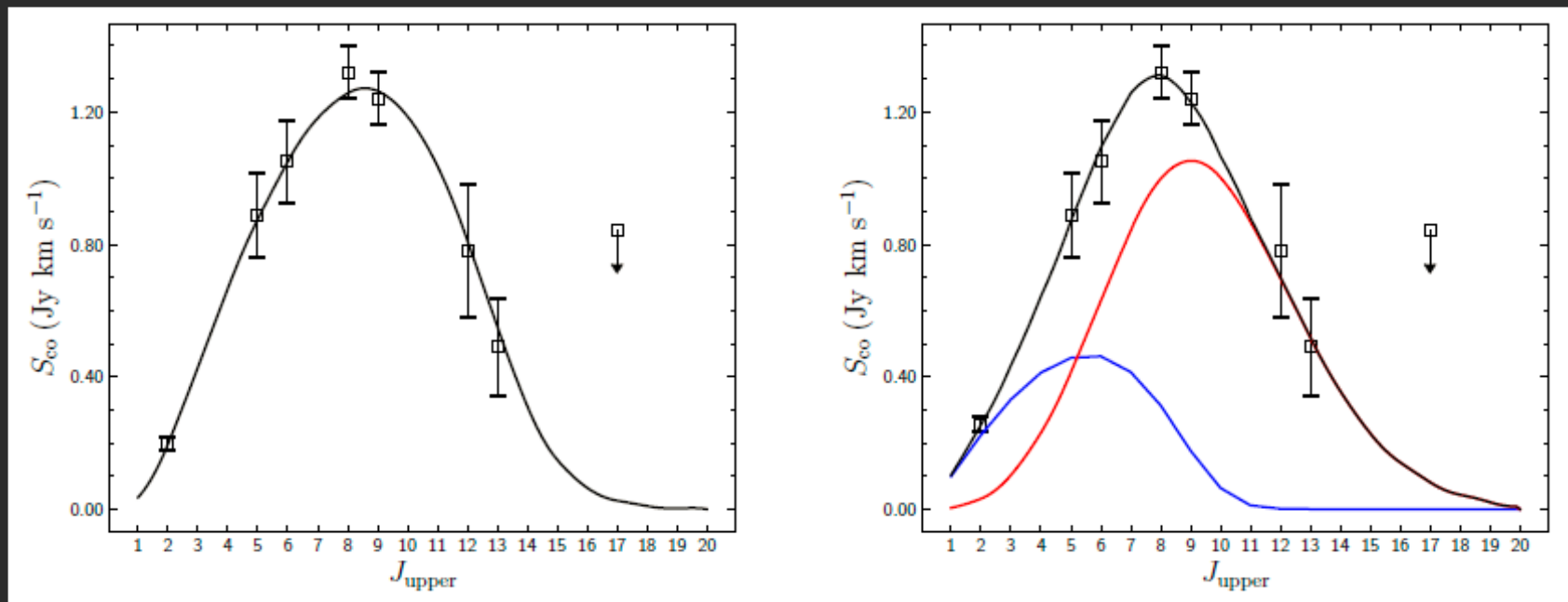


ALMA/NOEMA observations of the most FIR luminous object, Jianan Li et al.



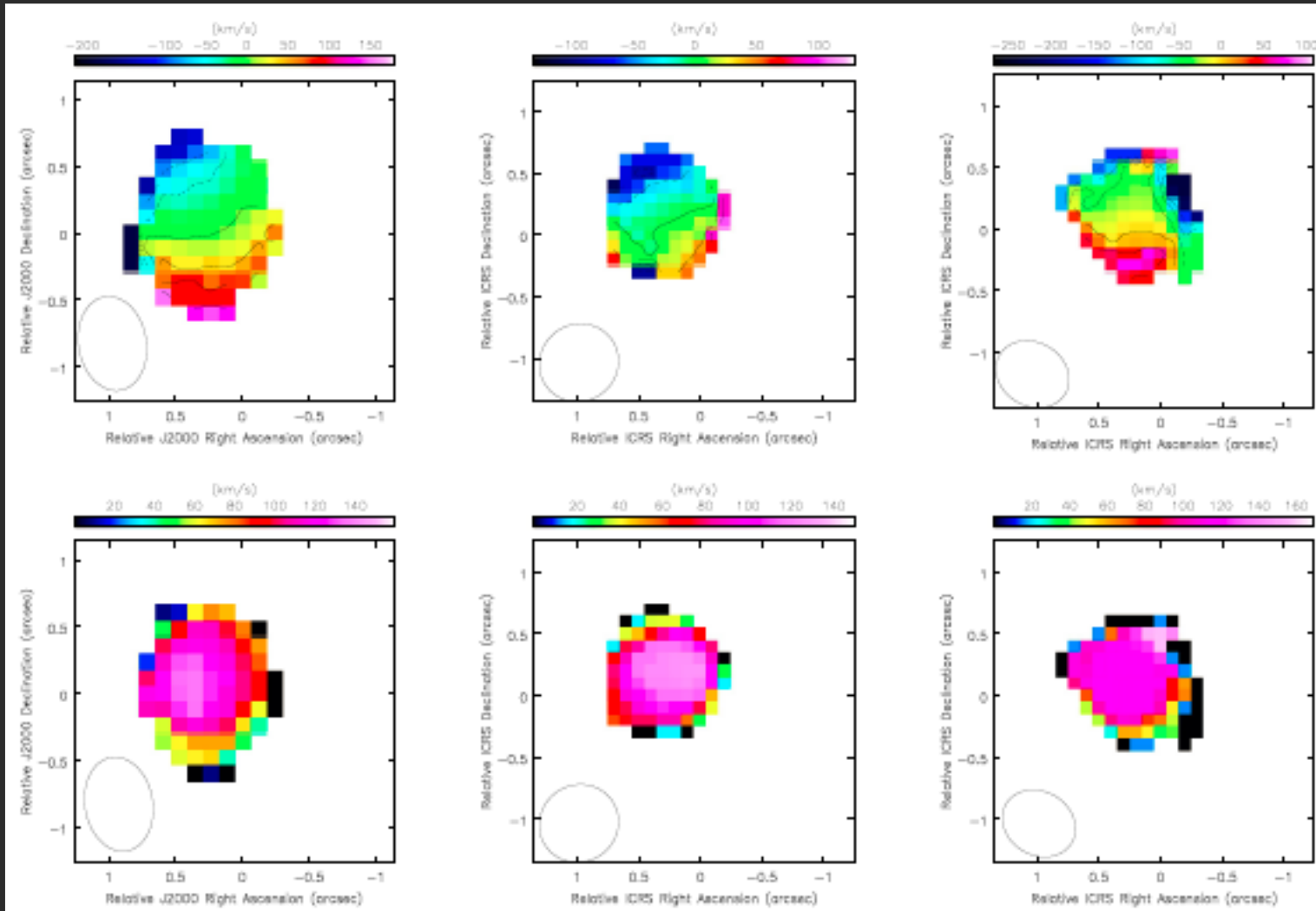
- SDSS J2310+1855, at $z=6.0$, FIR luminous with luminosity of $10^{13} L_{\odot}$;
- We search for CO (8-7) (9-8) line with ALMA, $\sim 0.6''$ resolution;
- CO (13-12), (12-11), (5-4) with NOEMA;
- Preliminary results : the CO SLED and molecular gas excitation;

- The CO SLED could be described with a single molecular gas component with the LVG model;
- Left : single component, $T_K \sim$ hundred K, $n(H_2) \sim 10^5 \text{ cm}^{-3}$;
- Right : double components, J1148 + hotter and denser component;



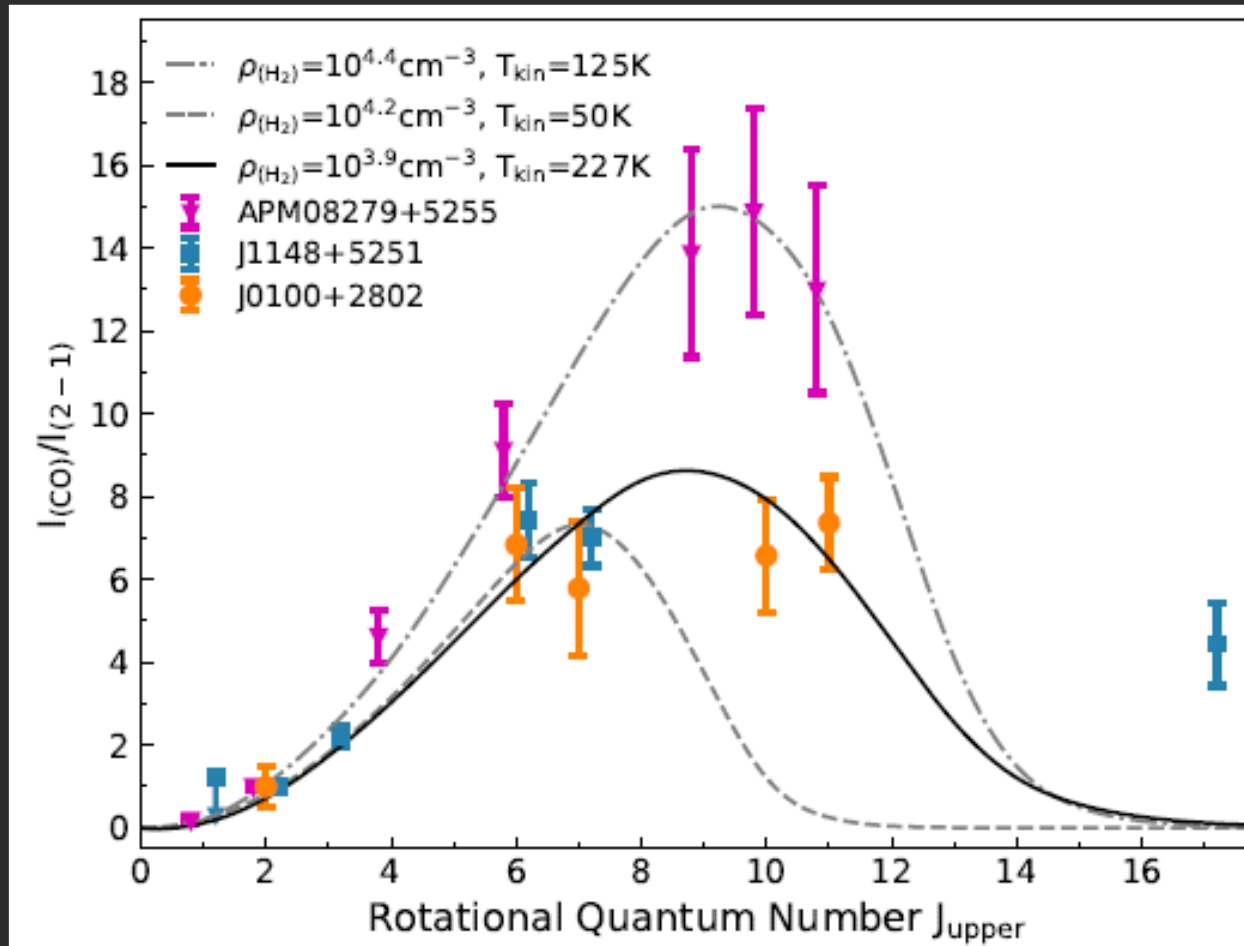
- The ALMA observation at 0.6" resolution, we are looking at the dense gas in the nuclear region;

- Velocity maps : compared between [C II], CO (8-7), CO (9-8), Li et al. 2019 to be submitted



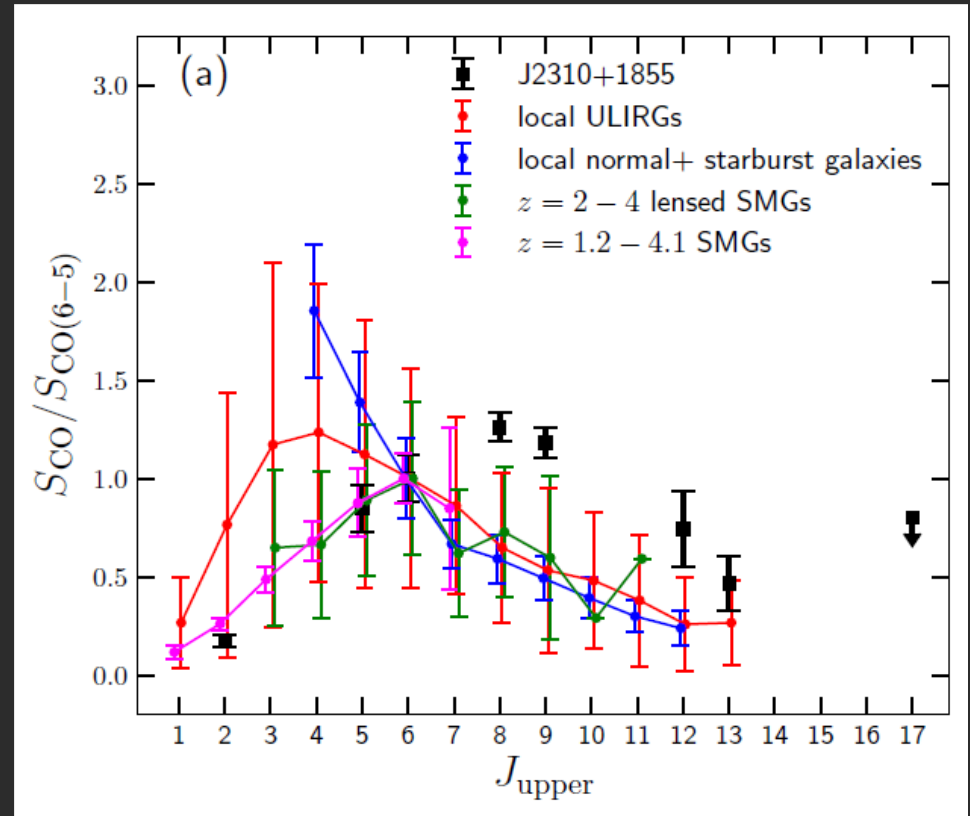
CO SLED of the most massive quasar J0100+2802 at $z=6.3$ Wang, F. et al. 2019

- Best fitted with two components:



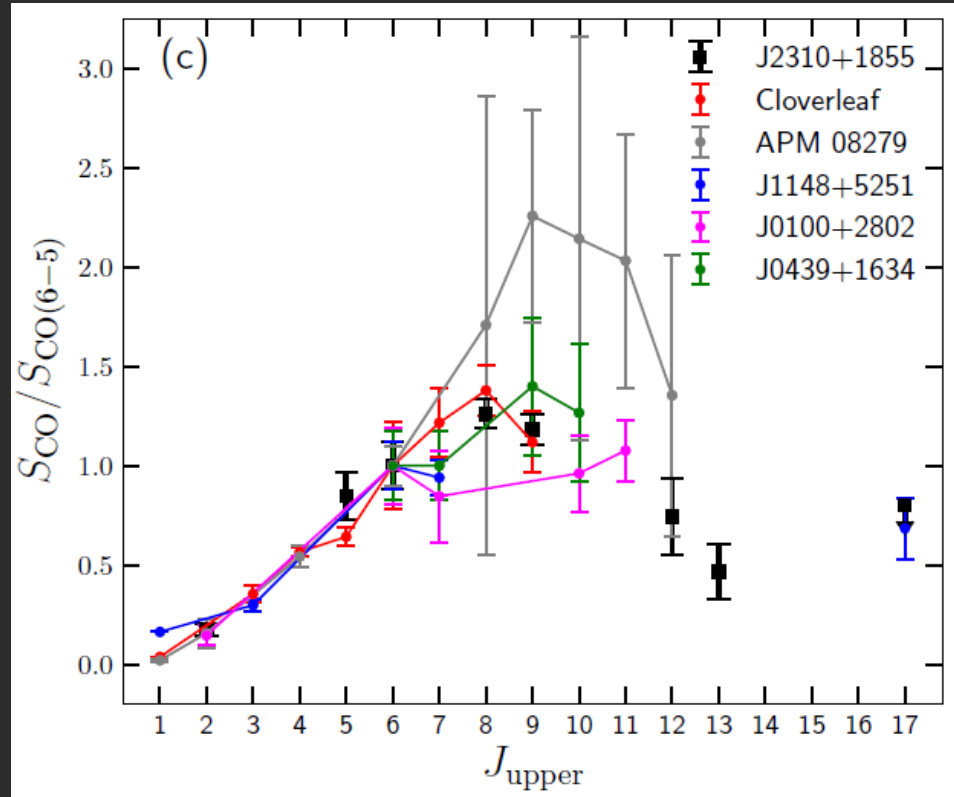
Physical condition and excitation of the ISM

- CO SLED of one of the mm bright $z \sim 6$ quasar (black square):
- Compared to the starburst systems.
- Highly excited molecular gas that dominated the high- J CO SLED.



Physical condition and excitation of the ISM

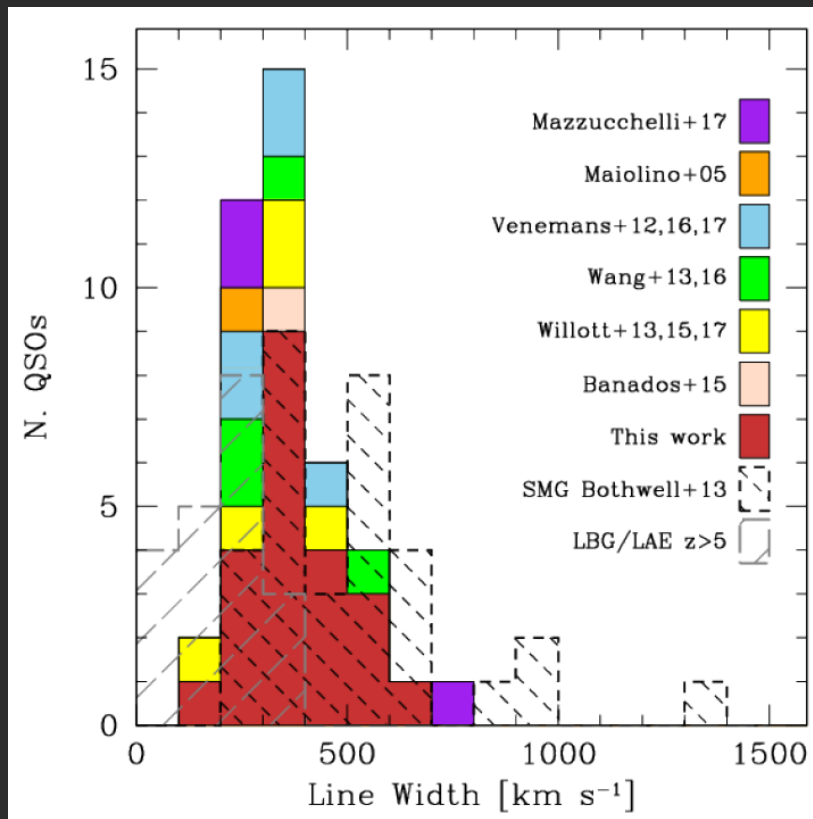
- CO SLED of quasar hosts, including four quasars at $z \sim 6$;
- Dense (10^5 cm^{-3}) and warm (10^2 K) molecular gas component that dominates the high- J transition;
- Powered by AGN ?
- Cold component associated with the 40-50 K dust ?



Li et al. 2019 submitted

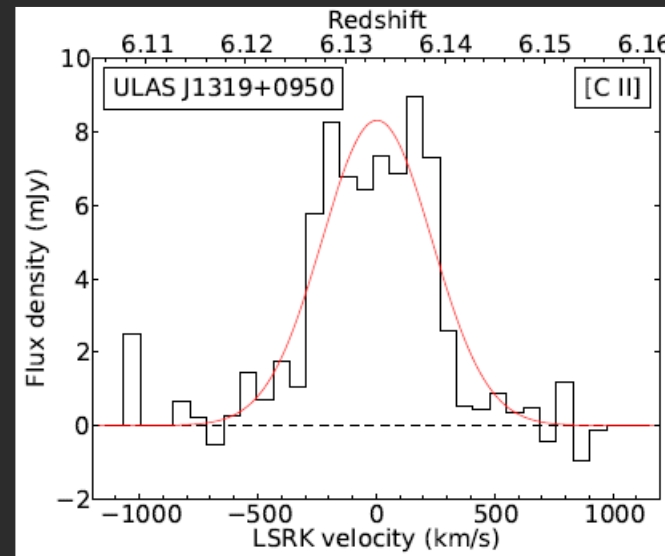
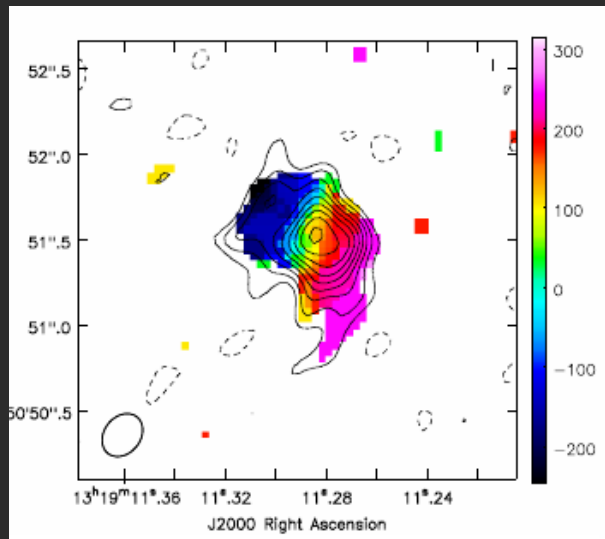
Gas kinematics

- Surveys of [CII] line in the $z \sim 6$ quasar hosts:
Similar [C II] line width distributions between quasars and SMGs (Decarli et al. 2018);



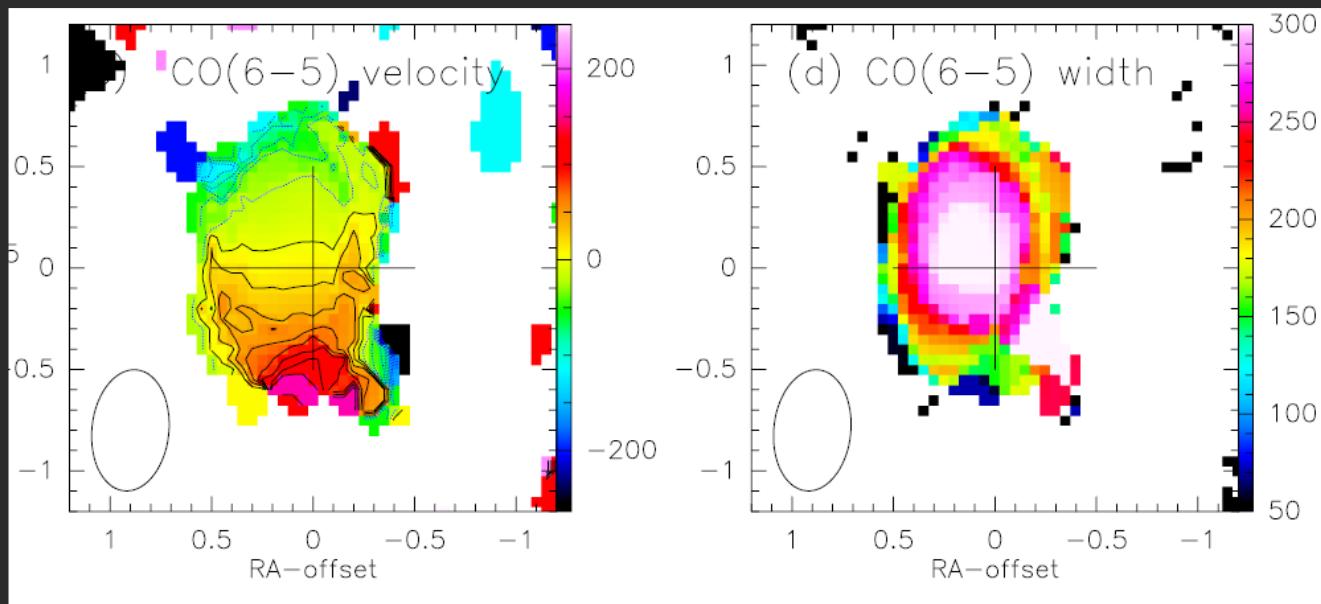
Gas kinematics - a range of activities

- Observations of the [C II] and CO emission lines from these young quasar hosts at $z>5.7$ at sub-arcsecond to arcsecond resolution reveal a range of kinematic properties:
- Velocity gradients: (Willott et al. 2013, 2017; Venemans et al. 2016; Shao et al. 2017) rotating motion.



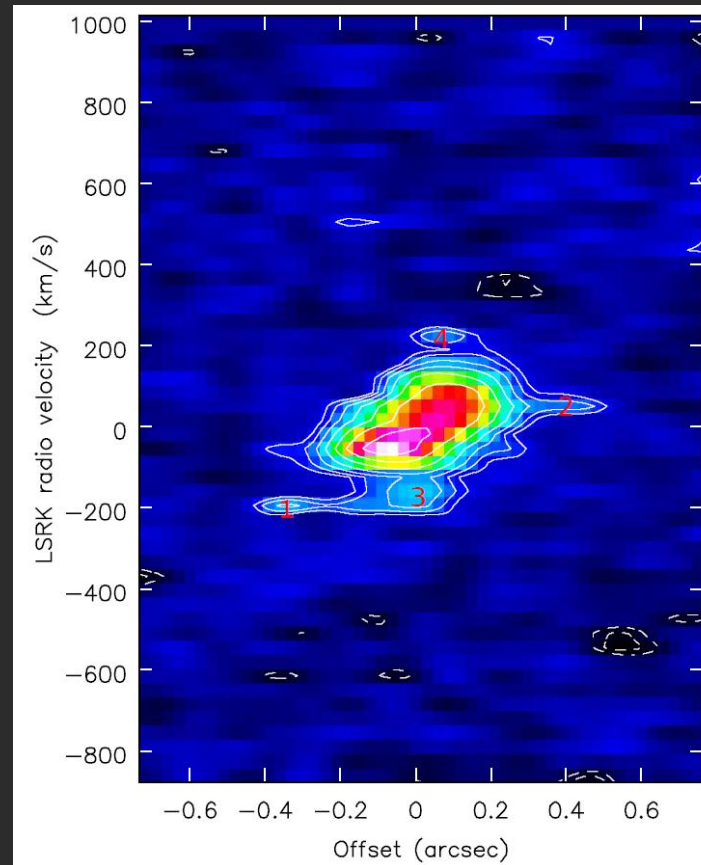
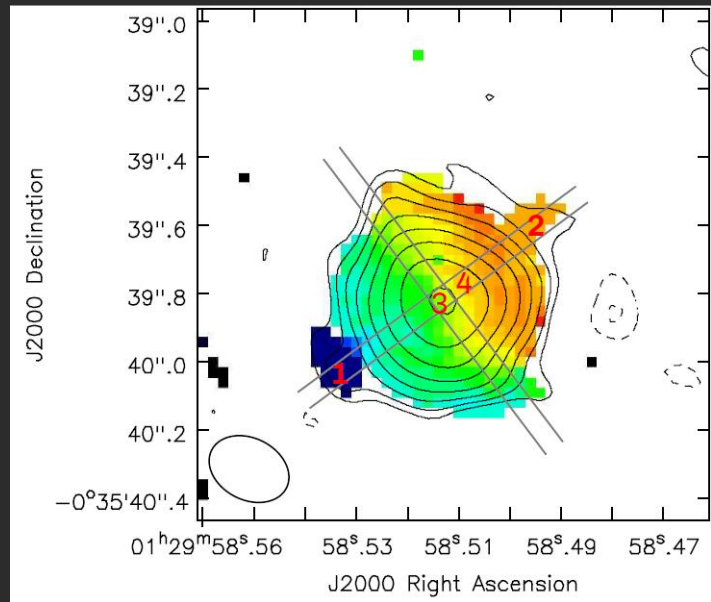
Gas kinematics - a range of activities

- Large velocity dispersion/turbulence
e.g., SDSS J2310+1855 at $z=6.0$, $v_{\text{rot}}/\sigma \sim 1-2$, Feruglio et al. 2018;



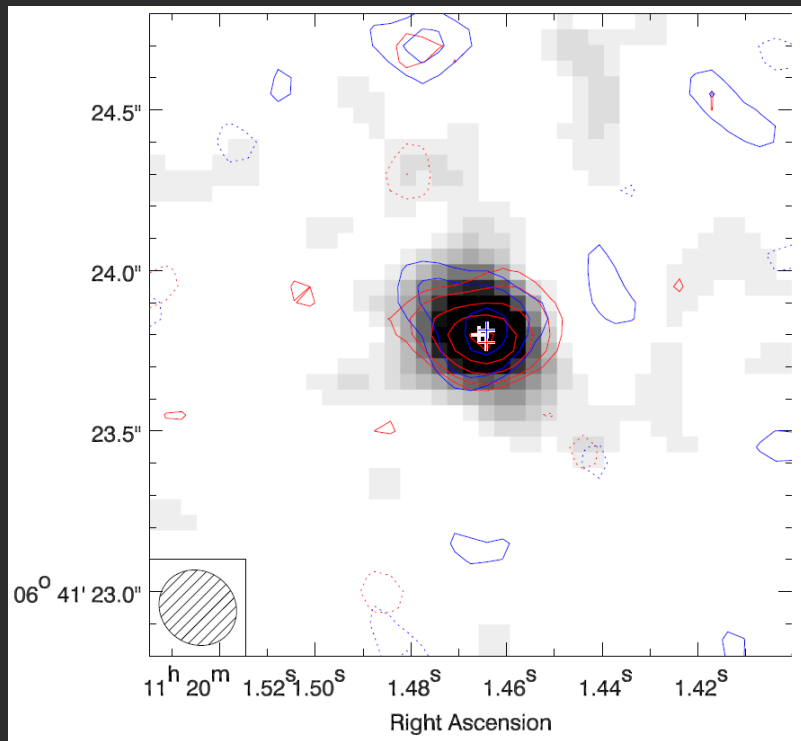
Gas kinematics - a range of activities

- SDSS J0129-0035 at $z=5.78$, complex gas kinematics, rotation + turbulent clumps (Wang et al. 2019)

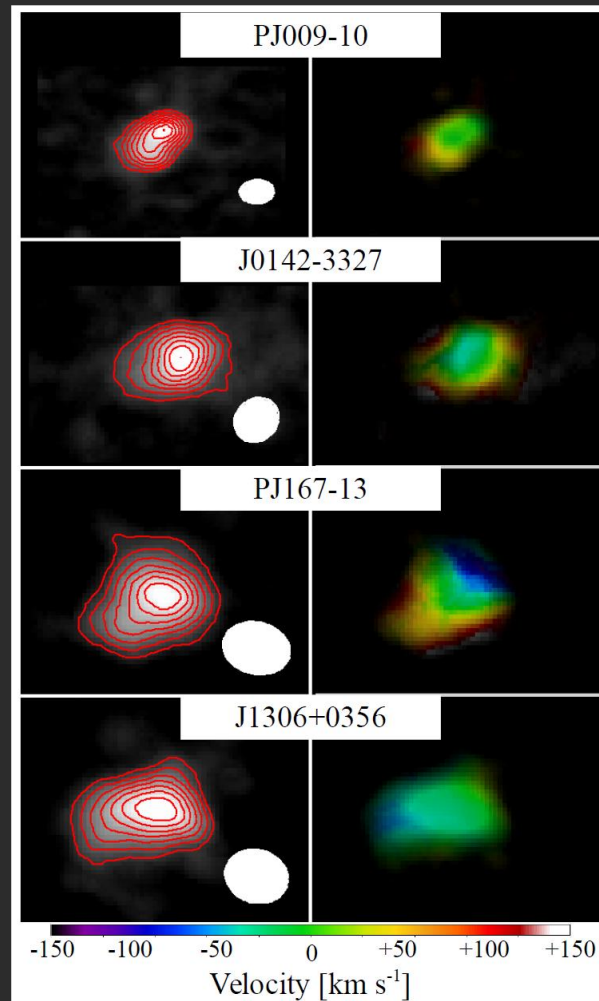


Gas kinematics - a range of activities

- Compact, dispersion-dominate system (Decarli et al. 2018; Venemans et al. 2018)

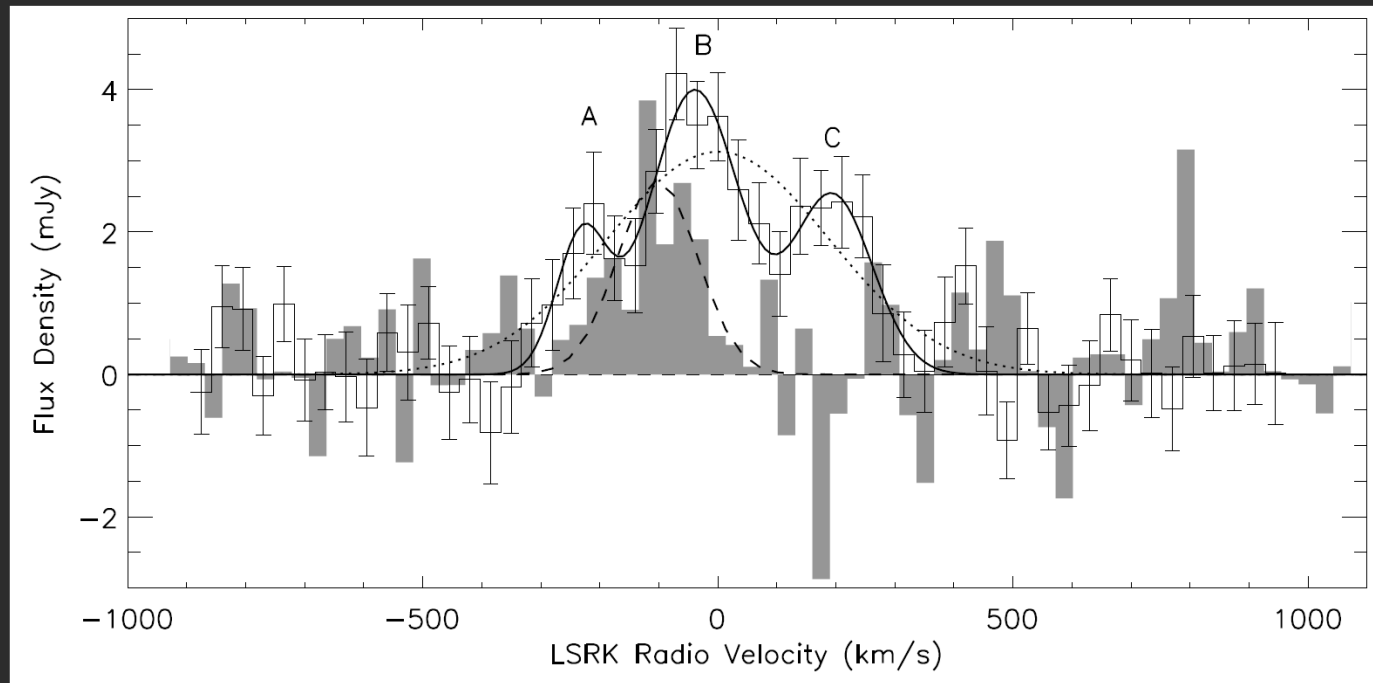


$z=7.1$ quasar, Venemans et al. 2017

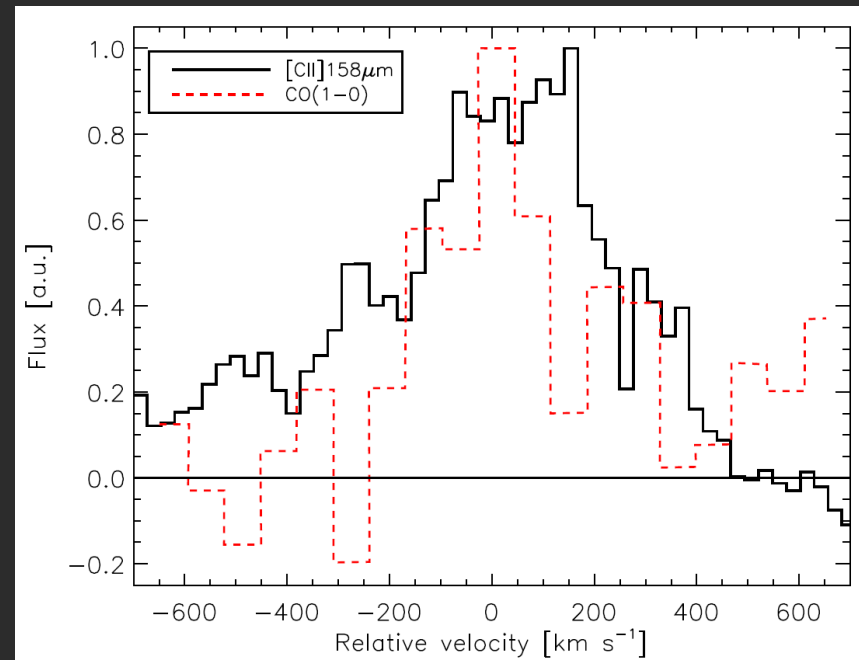


Different line profile between the [C II] and CO

- SDSS J1044-0125 at $z=5.78$, A warmer gas component traced by [C II] ?

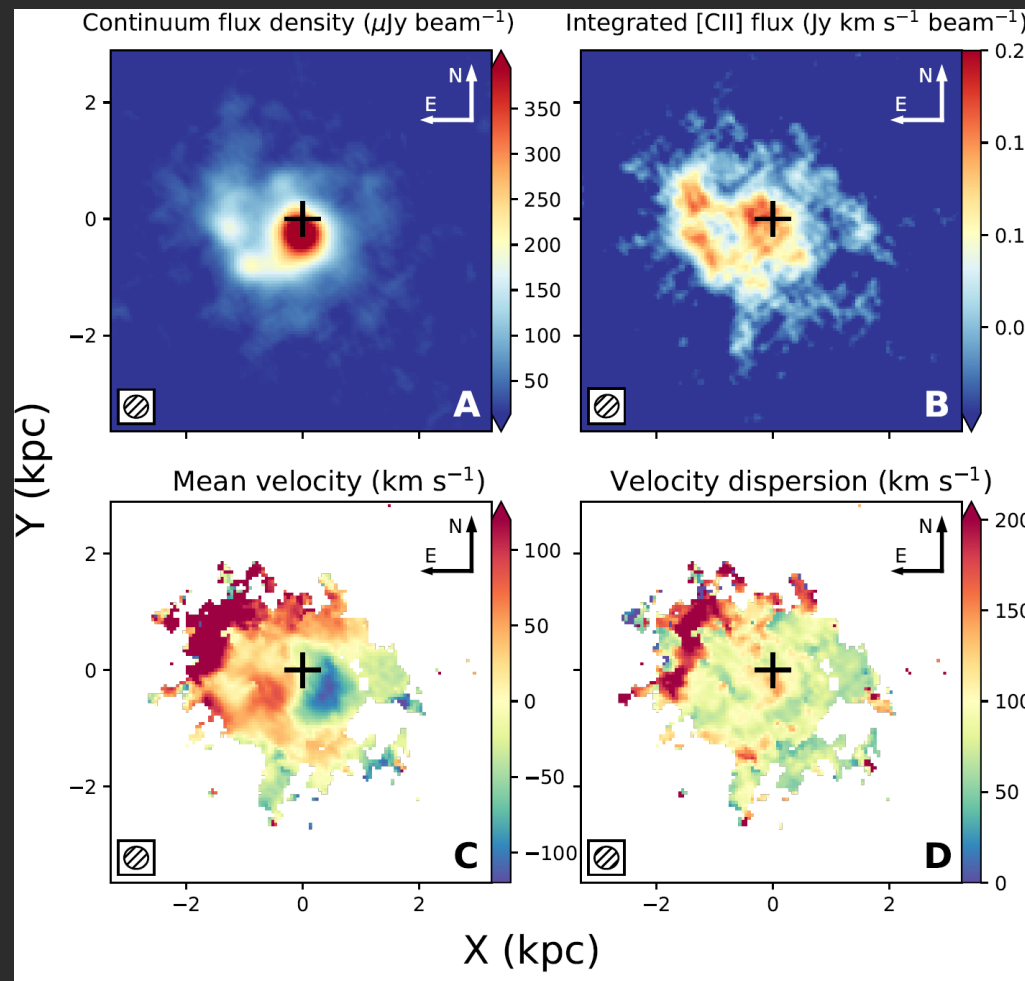


- CO(6-5) trace the dense molecular gas from star forming region;
- [C II] : trace the disk gas and star forming regions, as well as the warm diffuse neutral/ionized medium, could also powered by the central AGN;
- e.g., Asymmetric [C II] line emission that is broader than the molecular CO emission was detected the radio galaxy 3C 326N, suggest [C II] emission from a warm diffuse and turbulent molecular gas component powered by AGN-jet activity (Figure from Guillard et al. 2015).

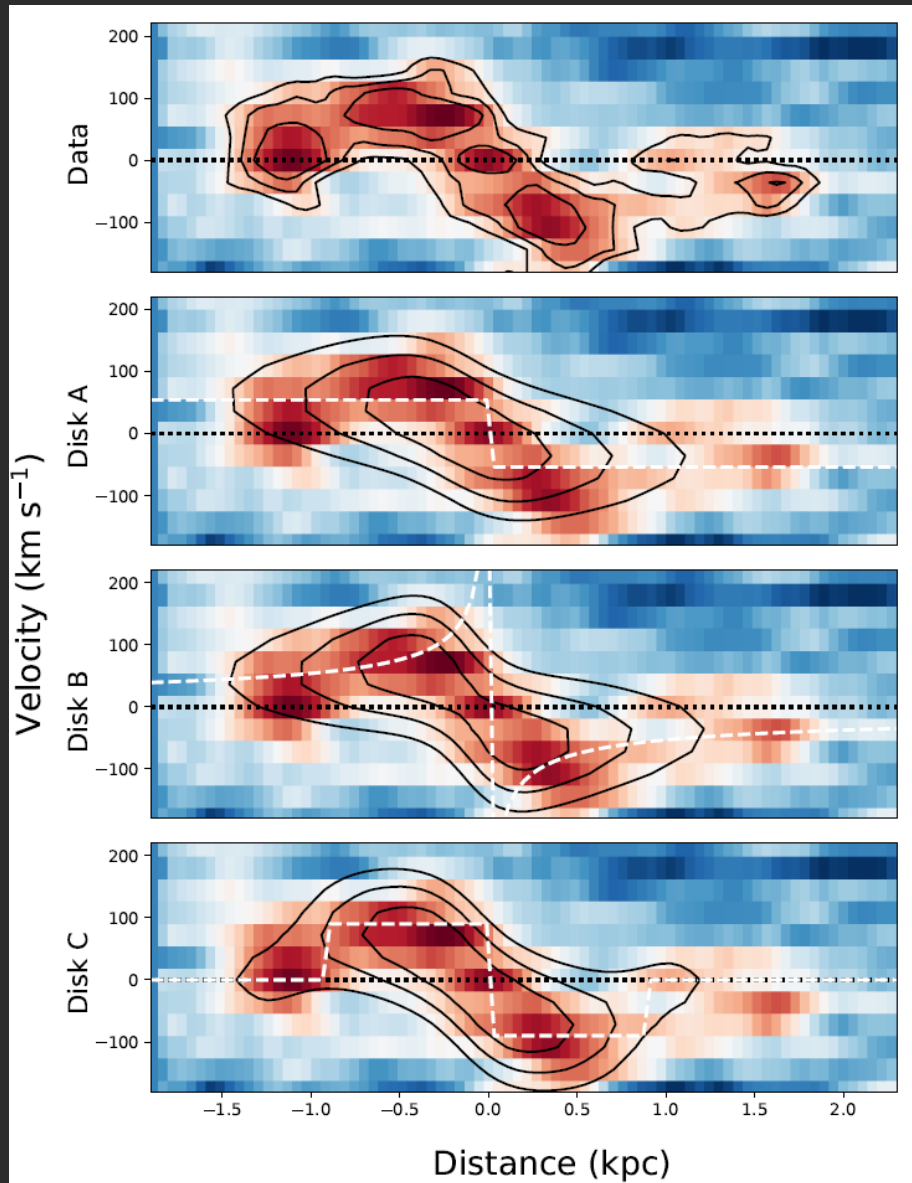


Gas kinematics - more details with ALMA image, recent work from Venemans et al. 2019

- 0.076" resolution with ALMA of a $z=6.6$ quasar host, Venemans et al. 2019;

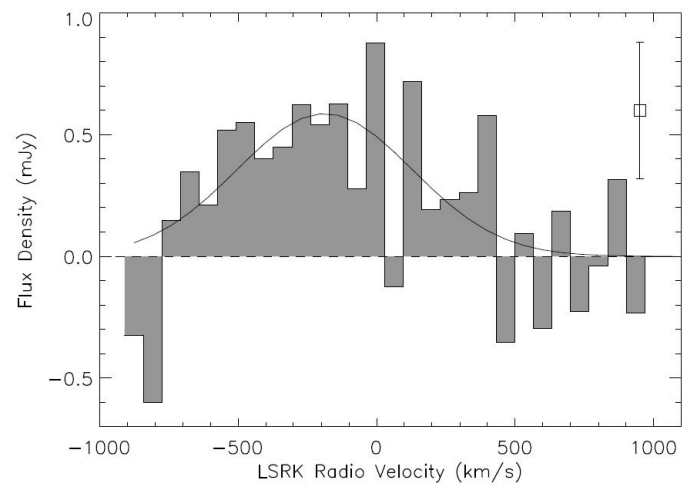
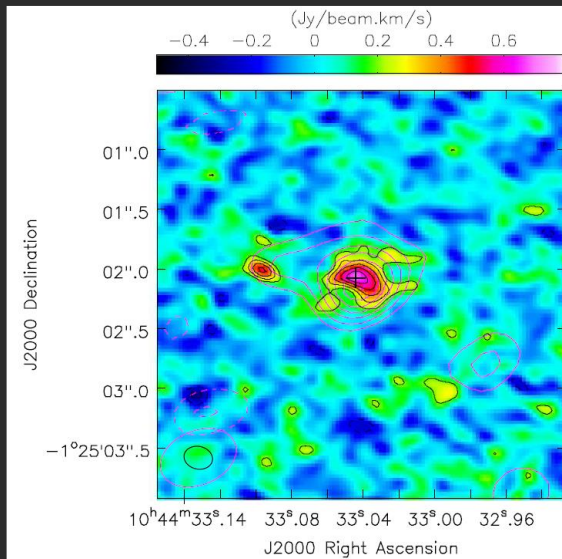


- Gas kinematics : dispersion + rotation in the central kpc.
- This implies that most of the gas has not yet settled in a disk ?
- Or heated/disrupted by the AGN ?



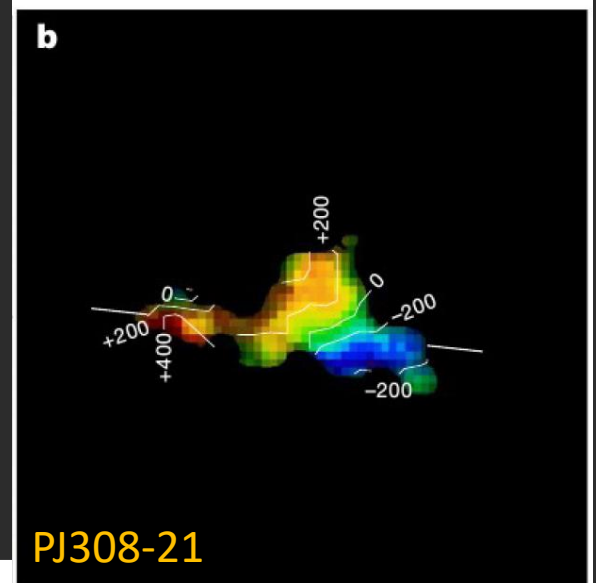
Gas kinematics - a range of activities

- Galaxy interactions/companions:
e.g., Decarli et al. 2017;



SDSS J1044-0125 at $z=5.78$, Wang et al. 2019

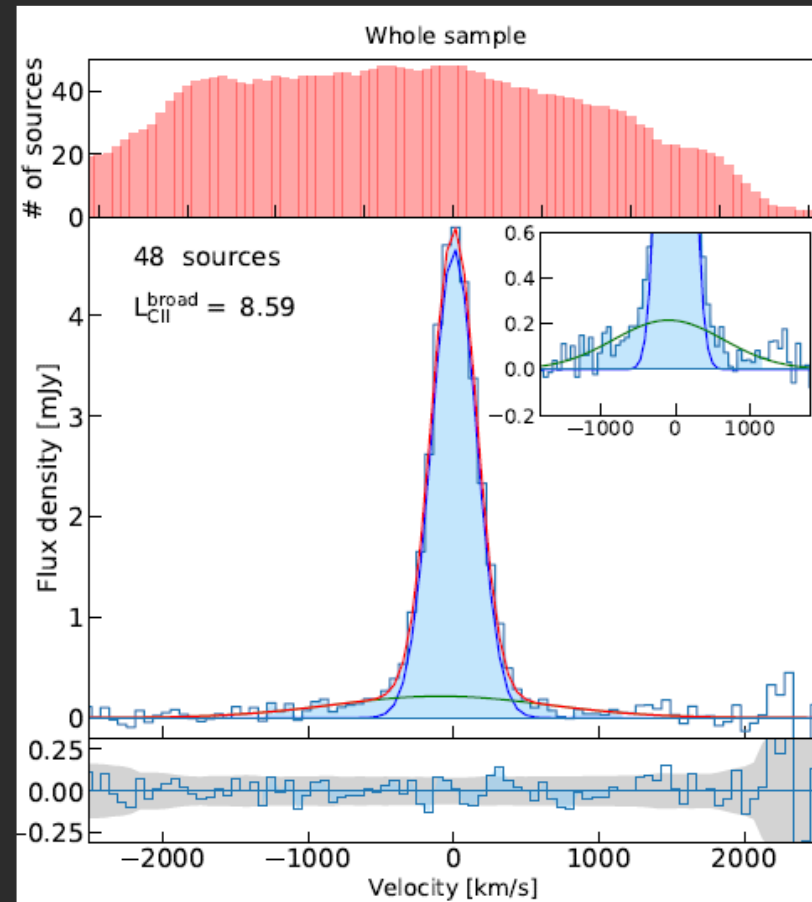
- Or gas outflows ?



Gas kinematics - a range of activities, recent work from Bischetti et al. 2018

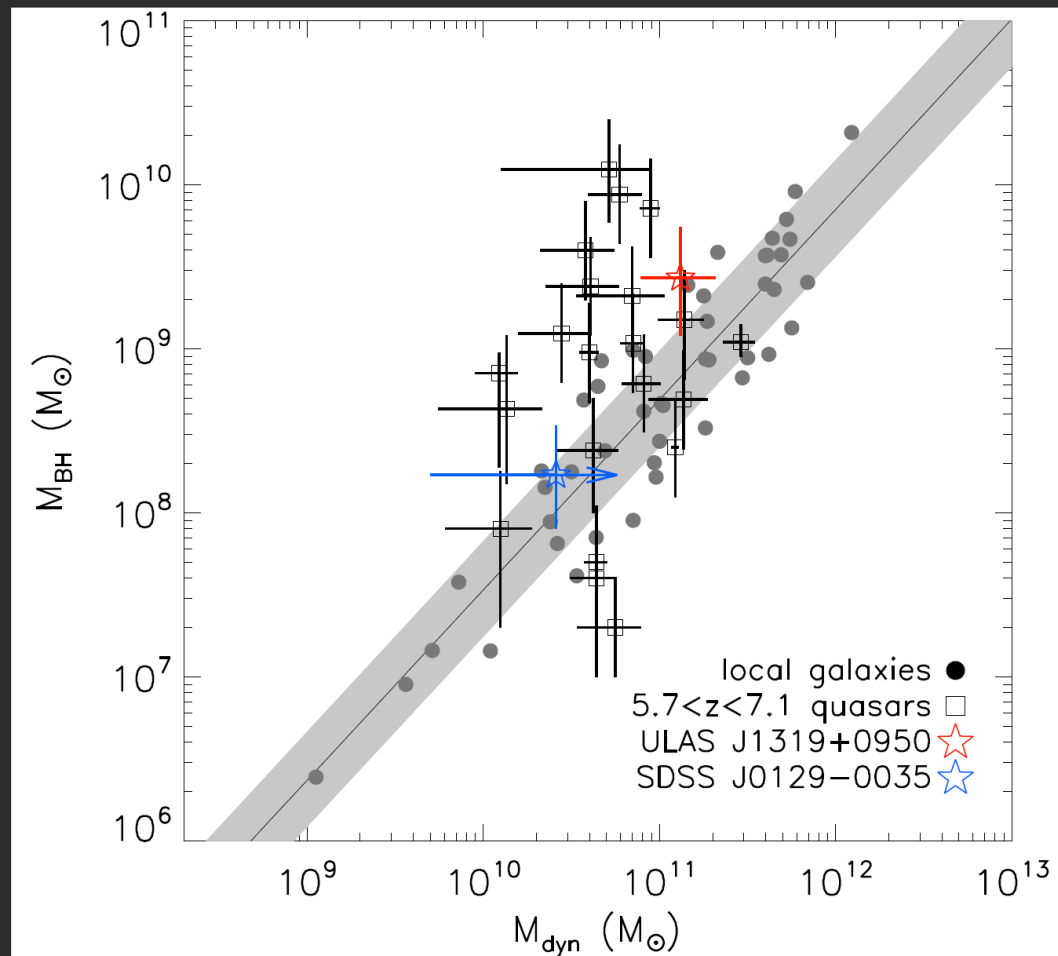
- Gas outflows: detections of low surface brightness, extended emission is indeed difficult.

Bischetti et al. 2018



$M_{\text{BH}} - M_{\text{dyn}}$: compared to local systems

- The dynamical mass constraints on these $z \sim 6$ to 7 quasars suggest that, in the early universe, the most massive SMBHs with masses of 10^9 to $10^{10} M_{\odot}$ may grow faster than that of their host galaxies (Walter et al. 2004; Venemans et al. 2016; Wang et al. 2016; Decarli et al. 2018);
- The less massive systems ($10^7 \sim 10^8 M_{\odot}$) are evolving more closer to the trend of local galaxies (Willott et al. 2017; Izumi et al. 2018).



Discussions: Dynamical mass of the quasar host

- Can the [C II], or CO emitting region trace the stellar component in the quasar hosts ?
- Line width from the observing spectrum → circular velocity (rotating system) / velocity dispersion (dispersion-dominated system);
- Uncertainties in the SMBH mass ;
- Will need JWST to directly image the stellar component.

Summary

- Large samples of quasars at $z>6$ are now selected from deep optical and near-IR surveys: these objects allow us to study the formation of the first SMBHs and galaxies;
- The mm and radio telescopes allow us to observe the dust and gas components in these earliest galaxies;
- Detections of strong dust continuum, molecular CO, [C II] in quasar host galaxies at $z\sim 6$ and higher provide evidence of massive star formation, co-eval with rapid SMBH accretion;
- Line and FIR luminosity ratios : physical conditions of the ISM.
- Spatially resolved dust and gas emission : provide constraints on the dynamics of the quasar host galaxies, and evidence of AGN feedback;
- Preliminary constraints on the $M_{\text{BH}}-M_{\text{bulge}}$ relationships.

Open questions and Opportunities

- Evolutionary connections between different systems at the highest redshift;
- Star formation and ISM excitation in different systems: quasar host galaxy, dusty starburst galaxy with no visible AGN, normal star forming galaxies;
- SMBH-galaxy co-evolution : M- σ relationships, accurate measurement of the host galaxy masses, stellar velocity dispersion; directly imaging of stellar component;
- Modern millimeter and radio facilities : provide the required spatial resolution and sensitivity to detect the faint continuum and line emission from the most distant galaxies;
- Together with future optical and near-IR telescopes, e.g., JWST, TMT, will fully probe the formation of the first galaxies.